

Supplementary information for: Vaccination strategies against RSV

**Dan Yamin^{1*}✉, Forrest K. Jones^{2*}, John P. DeVincenzo^{3,4,5}, Shai Gertler², Oren Kobiler⁶,
Jeffrey P. Townsend^{7,8}, Alison P. Galvani²**

*Contributed equally

¹ Department of Industrial Engineering, Faculty of Engineering, Tel Aviv University, Tel Aviv 69978, Israel

² Center for Infectious Disease Modeling and Analysis, School of Public Health, Yale University, 135 College St., New Haven, CT 06510, USA

³ Division of Infectious Diseases Department of Pediatrics, Health Sciences Center, University of Tennessee, Memphis, TN 38103

⁴ Department of Microbiology, Immunology, and Biochemistry, Tel Aviv University, Tel Aviv 69978, Israel Tel Aviv University, Tel Aviv 69978, Israel

⁵ Children's Foundation Research Institute at Le Bonheur Children's Hospital, Memphis, TN 38103

⁶ Department of Clinical Microbiology and Immunology, Sackler School of Medicine, Tel Aviv University, Tel Aviv 69978, Israel

⁷ Department of Biostatistics, School of Public Health, Yale University, 135 College St., New Haven, CT 06510, USA

⁸ Program in Computational Biology and Bioinformatics, Yale University, 300 George St., New Haven, CT 06520, USA

✉Direct correspondence to Dan Yamin, yamind@post.tau.ac.il

Contents

1. The model	1
1.1 The model without vaccination	1
1.2 The model with vaccination	3
2. Data set and parameters	7
2.1 Fixed parameters	7
2.2 Calibrated parameters	12
3. Calculation of secondary cases generated per infection	17
4. Additional results	18
5. Model and simulation analysis code in Mathematica 10	25

1. The model

1.1 The model without vaccination

We developed a dynamic model for age-stratified RSV infection progression and transmission in four states in the United States. Our model is a modified Susceptible-Infected-Recovered-Infected (SIRI) compartmental framework (1), whereby the population is stratified into health-related compartments, and transitions between the compartments occurs over time (Main text, Fig. 1; Fig. S1). To model age-dependent transmission, we stratified the population into $n = 8$ age groups: 0–5 months, 6–11 months, 1 year, 2–4 years, 5–24 years, 25–49 years, 50–64 years, and ≥ 65 years. Consistent with immunological observations (2, 3), and as in previous transmission models (4–7), we assumed individuals to be born with temporary protection conferred by maternal antibodies. Lifelong partial immunity is built up following the first infection, leading to 1) a lower susceptibility to infection (8), and 2) a lower viral load and severity in case of subsequent infection, which can be very mild or asymptomatic (9, 10) (see also, SI Appendix 2.1 Dataset and Parameters). With respect to subsequent infections, there is no evidence for immunity beyond that conferred by the partial immunity of a first infection. Protective short-term immunity following infection, however, has been observed (11).

Accordingly, we stratified the population into five health related compartments: maternally immune $M_j(t)$, susceptible $S_{k,j}(t)$, symptomatic infectious $I_{k,j}(t)$, asymptomatic infectious $A_j(t)$, and recovered $R_j(t)$, such that at any given time t (in days):

$$\sum_{j=1}^n \left[M_j(t) + \sum_{k=1}^2 \left(S_{k,j}(t) + I_{k,j}(t) \right) + A_j(t) + R_j(t) \right] = 1, \quad (1)$$

where the index $j \in \{1, 2, \dots, n\}$ represents the age group of each individual, and the index $k \in \{1, 2\}$ specifies the ordinality of the infection (i.e. first, or subsequent infection).

Model transitioning

Individuals are born at a birth rate Λ into compartment $M_{j=1}$, during which they are temporarily protected by maternal immunity for $1/w_M$ days (See Table S1). After this initial stage, they transition into the first susceptible compartment $S_{k=1,j}$, where they can become infected with a force of infection λ_j , depending on their age group j . Infected individuals remain in the infectious compartment $I_{k=1,j}$ for $\varphi_{k=1}$ days and can infect their contacts based on their daily viral load and daily contact behavior (Fig. 1b and SI Appendix 2.1 Data set and parameters). Following recovery, individuals transition into the second susceptible compartment $S_{k=2,j}$, where their susceptibility σ_j , is age-dependent. While asymptomatic RSV infection has not been detected in children below five years, RSV can be asymptomatic in adults (12). Thus, in individuals five years and over, we assumed infections after the first to be asymptomatic with probability α . In the case of asymptomatic infection, contact mixing is unaffected, but transmission is lower than during symptomatic infection due to a lower viral load (Main text, Fig. 1b and SI Appendix, 2.1 Data set and parameters).

To incorporate the evolution of infectiousness during infection, we explicitly track the number of symptomatic and asymptomatic infected individuals ($i_{k,j}^\tau, a_j^\tau$), respectively, with regard to their day of infection, τ . Hence, $I_{k,j} = \sum_{\tau=0}^{\varphi_k} i_{k,j}^\tau$ and $A_j = \sum_{\tau=0}^{\varphi_{k=2}} a_j^\tau$. Demographically, individuals in age group j transition within their compartment to age group $j + 1$ at rate d_j , and die at a rate μ_j , such that the total population and age-structure remain constant. In the US, death due to RSV is uncommon relative to the overall death rate. Therefore, its effect on transmission is negligible, and is not explicitly included in our model. Thus, with no vaccination, the transmission model is composed of the following system of difference equations:

$$\begin{aligned}
M_j(t) - M_j(t-1) &= \delta_{j,1} \cdot \Lambda + d_{j-1}M_{j-1}(t-1) - (d_j + \mu_j + w_M)M_j(t-1), \\
S_{k=1,j}(t) - S_{k=1,j}(t-1) &= d_{j-1}S_{k=1,j-1}(t-1) + w_M M_j(t-1) - (d_j + \mu_j + \lambda_j)S_{k=1,j}(t-1), \\
S_{k=2,j}(t) - S_{k=2,j}(t-1) &= d_{j-1}S_{k=2,j-1}(t-1) - (d_j + \mu_j + \sigma_{k=2,j}\lambda_j)S_{k=2,j}(t-1) + \\
&\quad w_R R_{j-1}(t-1), \\
R_j(t) - R_j(t-1) &= d_{j-1}R_{j-1}(t-1) + (1 - \mu_j) \left(a_j^{\tau=\varphi_{k=2}}(t-1) + \sum_{k=1}^2 i_{k,j}^{\tau=\varphi_k}(t-1) \right) - \\
&\quad (d_j + \mu_j)R_j(t-1) - w_R R_{j-1}(t-1),
\end{aligned} \tag{2}$$

with daily numbers of infected individuals:

$$\begin{aligned}
i_{k=1,j}^{\tau=0}(t) &= \lambda_j(t)S_{k=1,j}(t-1), \\
i_{k=2,j}^{\tau=0}(t) &= (1 - \alpha)\sigma_j\lambda_j(t)S_{k=2,j}(t-1), \\
i_{k,j}^{\tau \neq 0}(t) &= d_{j-1}i_{k,j-1}^{\tau-1}(t-1) + (1 - d_j - \mu_j)i_{k,j}^{\tau-1}(t-1), \\
a_j^{\tau=0}(t) &= \alpha\sigma_j\lambda_j(t)S_{k=2,j}(t-1), \\
a_j^{\tau \neq 0}(t) &= d_{j-1}a_{j-1}^{\tau-1}(t-1) + (1 - d_j - \mu_j)a_j^{\tau-1}(t-1).
\end{aligned} \tag{3}$$

The term $\delta_{i,j}$ is the Kronecker delta, such that $\delta_{j,1}$ equals unity for the first age group, and zero otherwise. In accordance with our model assumptions, we set:

$$M_0(t) = S_{k,0}(t) = i_{k,0}^{\tau}(t) = a_0^{\tau}(t) = R_0(t) = 0 \quad \forall t, k, \tau. \tag{4}$$

Force of infection

The rate at which an individual acquires infection at time t is $\lambda_j(t)$ for first infection, and $\sigma_j\lambda_j(t)$ for subsequent infections. This force of infection for RSV depends on a combination of 1) seasonality, 2) infectiousness of the infected contact, and 3) susceptibility of individuals.

Peak incidence of RSV typically strikes during the winter in the US (13), yet the driver for this seasonality remains unclear (7). Thus, we included general seasonal variation in the susceptibility rate of the model

$$T(t) = \Gamma * \left(1 + \cos \left[\frac{2\pi}{365} (t - \phi) \right] \right), \tag{5}$$

in which Γ is the seasonal amplitude, and ϕ is a seasonal offset. This formulation was previously demonstrated to accurately capture the seasonal variations of RSV incidence by US state (7).

We incorporated age-specific contact patterns between individuals, represented by a data-driven contact rate between an infected individual in age-group e and each of their susceptible contacts in age-group j , denoted $C_{e,j}$ (see 2. Data set and Parameters) (14). Symptomatic infection might lead to withdrawal from social activities, particularly in the days of infection for which viral load is highest (Main text, Fig. 1b). Thus, we assign the daily probability of withdrawal from social activity, for an individual from age group j , to be $\psi_j(\tau)$. As RSV typically results in mild infection among healthy adults (10), withdrawal from social activity is less likely in adults, but could occur mainly during the three days surrounding the time of peak viral load (Main text, Fig. 1B). To incorporate the per-day mixing patterns of those who withdraw from

social interaction while infected, we set the number of contacts from their age group to zero, but assumed that the number of contacts with people from different age groups is unaffected.

Given a contact with an infected host, the logarithm of the infectious viral load has been shown to be correlated to the transmissibility of several respiratory viruses, including RSV (15–17). The viral load depends on both on the immunity that the infected individual acquired from the first exposure k , and also on whether the infection is symptomatic or asymptomatic (Main text, Fig. 1b). Taken together, the force of infection $\lambda_j(t)$ is given by:

$$\lambda_j(t) = T(t) \left(\sum_{k=1}^2 \sum_{\tau=0}^{\varphi_k} \left[(r^{\log[V_k(\tau)]} - 1) \sum_{e=1}^n C_{e,j} (1 - \psi_n(\tau) \mathbb{I}_{e,j}) i_{k,e}^{\tau}(t) \right] + \sum_{\tau=0}^{\varphi_{k=2}} \left[(r^{\log[V_a(\tau)]} - 1) \sum_{e=1}^n C_{e,j} (1 - \psi_n(\tau) \mathbb{I}_{e,j}) a_e^{\tau}(t) \right] \right), \quad (6)$$

where \mathbb{I} is the 8×8 identity matrix. In this formulation, every 10-fold increase in the viral load corresponds to r -fold increase in transmission. The daily viral loads of infected individuals in compartments $i_{k,j}^{\tau}$ and a_j^{τ} are denoted $V_k(\tau)$ and $V_a(\tau)$ respectively.

1.2 The model with vaccination

RSV vaccines under development fall into two categories: replicating or non-replicating candidates. The latter tends to elicit only a systemic response and not a mucosal response, whereas the former stimulates both. Recent clinical data that measured immune markers in volunteers experimentally exposed to RSV (18, 19) demonstrated that both IgA (which mimics response to the live attenuated vaccine) and serum neutralizing antibodies (which mimics response to the inactivated vaccine) reduced susceptibility to infection. Depending on the efficacy of the vaccine, a proportion of people vaccinated are transitioned to a recovered compartment. For the remaining proportion, the immunological status of vaccinated individuals – those who have been ineffectively vaccinated – will be unaffected. To ensure individuals will not get vaccinated more than once in a season, susceptible individuals who were efficaciously vaccinated transition to an RV_I compartment, whereas individuals for whom the vaccine was ineffective transition to a compartment which represents the same epidemiological status prior to vaccination, but distinguishes them as ‘already vaccinated’ in the season (e.g. M to MV and S to SV , Figure S1).

Accordingly, for the model with vaccination, we stratified the population into nine health and vaccine related compartments: maternally immune $M_j(t)$, susceptible $S_{k,j}(t)$, symptomatic infectious $I_{k,j}(t)$, asymptomatic infectious $A_j(t)$, recovered $R_j(t)$, in addition to four compatible compartments for those who were vaccinated, maternally immune $MV_j(t)$, susceptible $SV_{k,j}(t)$, symptomatic infectious $IV_{k,j}(t)$, and asymptomatic infectious $AV_j(t)$, such that at any given time t (in days):

$$\sum_{j=1}^n \left[M_j(t) + MV_j(t) + \sum_{k=1}^2 (S_{k,j}(t) + SV_{k,j}(t) + I_{k,j}(t) + IV_{k,j}(t)) + A_j(t) + AV_j(t) + R_j(t) + RV_j(t) \right] = 1. \quad (7)$$

Although there are 16 ongoing clinical trials that target different age groups (20), the duration of protection for the vaccine remains uncertain. Nevertheless, it is likely that RSV vaccine will be provided annually given the short-term immunity following RSV infection (11), as well as provisional plans to administer the RSV vaccine together with the seasonal influenza vaccine (22). Hence, at the end of an RSV season, we stipulate that all individuals return to the compatible compartment (e.g. transition from MV_j to M_j , and from $SV_{k,j}$ to $S_{k,j}$) (Fig. S1). This transition at the end of each RSV season was obtained by defining a waning

rate, $w_V(t-1)$ with a fairly rapid waning rate at the end of an RSV season, ensuring that the proportion of individuals in the vaccinated compartments to be negligible before the beginning of the succeeding RSV season.

To parameterize the daily rate of vaccination for each group, $p_j(t)$, we used state-specific influenza vaccine coverage estimates (21) (see SI Appendix 2.1). Including vaccination, the transmission model is composed of the following system of difference equations:

$$\begin{aligned}
M_j(t) - M_j(t-1) &= \delta_{j,1} \cdot \Lambda + d_{j-1}M_{j-1}(t-1) - (d_j + \mu_j + w_M + p_j(t-1))M_j(t-1) + w_V(t-1)MV_j(t-1), \\
S_{k=1,j}(t) - S_{k=1,j}(t-1) &= d_{j-1}S_{k=1,j-1}(t-1) + w_M M_j(t-1) - (d_j + \mu_j + \lambda_j + p_j(t-1))S_{k=1,j}(t-1) + w_V(t-1)SV_{k=1,j}(t-1), \\
S_{k=2,j}(t) - S_{k=2,j}(t-1) &= d_{j-1}S_{k=2,j-1}(t-1) - (d_j + \mu_j + \sigma_j \lambda_j + p_j(t-1))S_{k=2,j}(t-1) + w_R R_{j-1}(t-1) + w_V(t-1)SV_{k=2,j}(t-1), \\
R_j(t) - R_j(t-1) &= d_{j-1}R_{j-1}(t-1) + (1 - \mu_j) \left(\sum_{k=1}^2 i_{k,j}^{\tau=\varphi_k}(t-1) + a_j^{\tau=\varphi_{k=2}}(t-1) \right) - (d_j + \mu_j)R_j(t-1) - w_R R_{j-1}(t-1) - p_j(t-1)R_j(t-1) + w_V(t-1)RV_{j-1}(t-1), \\
MV_j(t) - MV_j(t-1) &= d_{j-1}MV_{j-1}(t-1) - (d_j + \mu_j + w_M + w_V(t-1))MV_j(t-1) + (1 - v_j)p_j(t-1)MV_j(t-1), \\
SV_{k=1,j}(t) - SV_{k=1,j}(t-1) &= d_{j-1}SV_{k=1,j-1}(t-1) + w_M VM_j(t-1) - (d_j + \mu_j + \lambda_j + w_V(t-1))SV_{k=1,j}(t-1) + (1 - v_j)p_j(t-1)S_{k=1,j}(t-1), \\
SV_{k=2,j}(t) - SV_{k=2,j}(t-1) &= d_{j-1}SV_{k=2,j-1}(t-1) - (d_j + \mu_j + \sigma_j \lambda_j + w_V(t-1))SV_{k=2,j}(t-1) + w_R V_{j-1}(t-1) + (1 - v_j)p_j(t-1)S_{k=2,j}(t-1), \\
RV_j(t) - RV_j(t-1) &= d_{j-1}RV_{j-1}(t-1) + (1 - \mu_j) \left(\sum_{k=1}^2 iv_{k,j}^{\tau=\varphi_k}(t-1) + av_j^{\tau=\varphi_{k=2}}(t-1) \right) - (d_j + \mu_j)RV_j(t-1) - w_R RV_{j-1}(t-1) + v_j p_j(t-1) \left(M_j(t-1) + S_{k=1,j}(t-1) + S_{k=2,j}(t-1) \right) + p_j(t-1)R_j(t-1) - w_V(t-1)RV_{j-1}(t-1),
\end{aligned} \tag{8}$$

with a daily number of infected individuals:

$$\begin{aligned}
i_{k=1,j}^{\tau=0}(t) &= \lambda_j(t)S_{k=1,j}(t-1), \\
i_{k=2,j}^{\tau=0}(t) &= (1 - \alpha)\sigma_j \lambda_j(t)S_{k=2,j}(t-1), \\
i_{k,j}^{\tau \neq 0}(t) &= d_{j-1}i_{k,j-1}^{\tau-1}(t-1) + (1 - d_j - \mu_j)i_{k,j}^{\tau-1}(t-1), \\
a_j^{\tau=0}(t) &= \alpha\sigma_j \lambda_j(t)S_{k=2,j}(t-1), \\
a_j^{\tau \neq 0}(t) &= d_{j-1}a_{j-1}^{\tau-1}(t-1) + (1 - d_j - \mu_j)a_j^{\tau-1}(t-1), \\
iv_{k=1,j}^{\tau=0}(t) &= \lambda_j(t)SV_{k=1,j}(t-1), \\
iv_{k=2,j}^{\tau=0}(t) &= (1 - \alpha)\sigma_j \lambda_j(t)SV_{k=2,j}(t-1),
\end{aligned} \tag{9}$$

$$iv_{k,j}^{\tau \neq 0}(t) = d_{j-1}iv_{k,j-1}^{\tau-1}(t-1) + (1 - d_j - \mu_j)iv_{k,j}^{\tau-1}(t-1),$$

$$av_j^{\tau=0}(t) = \alpha\sigma_j\lambda_jSV_{k=2,j}(t-1),$$

$$av_j^{\tau \neq 0}(t) = d_{j-1}av_{j-1}^{\tau-1}(t-1) + (1 - d_j - \mu_j)av_j^{\tau-1}(t-1),$$

where $iv_{k,j}^{\tau}(t)$ ($av_{k,j}^{\tau}(t)$) represents for time t , the number of individuals from age group j that were vaccinated and are in their τ^{th} day of infection of type k (i.e. symptomatic or asymptomatic). Similar to the model with no vaccination, we set:

$$M_0(t) = S_{k,0}(t) = SV_{k,0}(t) = i_{k,0}^{\tau}(t) = a_0^{\tau}(t) = iv_{k,0}^{\tau}(t) = av_0^{\tau}(t) = R_0(t) = 0 \forall t, k, \tau. \quad (10)$$

The corresponding force of infection is:

$$\lambda_j(t) = T(t) \left(\sum_{k=1}^2 \sum_{\tau=0}^{\varphi_k} \left[(r^{\log[V_k(\tau)]} - 1) \sum_{e=1}^n C_{e,j} (1 - \psi_e(\tau) \mathbb{I}_{e,j}) (i_{k,e}^{\tau}(t) + iv_{k,e}^{\tau}(t)) \right] \right. \\ \left. + \sum_{\tau=0}^{\varphi_{k=2}} \left[(r^{\log[V_a(\tau)]} - 1) \sum_{e=1}^n C_{e,j} (1 - \psi_e(\tau) \mathbb{I}_{e,j}) (a_e^{\tau}(t) + av_e^{\tau}(t)) \right] \right). \quad (11)$$

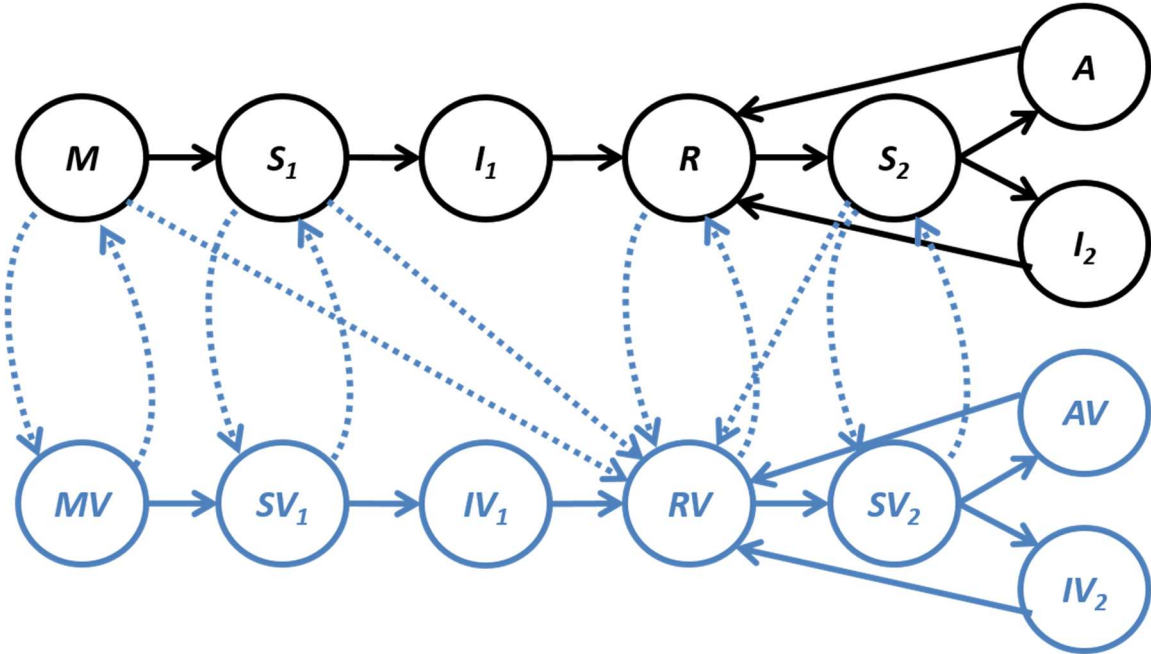


Fig. S1. Transmission model diagram with vaccination. Compartmental diagram of the transmission model without vaccination (black) and with vaccination (black and blue). Individuals are born into a maternal immunity compartment M , then transition to the first susceptible compartment S_1 , where they can become infected, I_1 . Following infection, individuals transition to a recovered compartment R , where they are temporarily protected. Following waning, individuals transition to S_2 , where they can be re-infected, but with milder infection I_2 , which can be asymptomatic in adults, A . Each vaccine can be either efficacious or inefficacious: efficacious vaccines mimics infection by transitioning susceptible

individuals to the Recovered Vaccinated (RV) compartment. Namely, to ensure individuals will not get vaccinated more than once in a season, 1) susceptible individuals who were efficaciously vaccinated transition to an RV compartment, whereas susceptible individuals for whom the vaccine was inefficacious transition to the SV_1 or SV_2 compartments, 2) individuals in maternal immunity compartment M , who were efficaciously vaccinated transition to an RV compartment, whereas individuals in maternal immunity compartment for whom the vaccine was inefficacious transition to the MV compartment, and 3) individuals in the recovered compartment R , will move to the RV compartment. At the end of RSV season, all individuals return to the compatible compartment (i.e. MV to M , SV_1 to S_1 , IV_1 to I_1 , RV to R). For clarity of depiction, age classes stratifications are not displayed.

2. Data set and parameters

2.1 Fixed parameters

We parameterized the age-specific contact rates between an infected individual e and their contact j , $C_{e,j}$, using data from a survey of daily contacts collected in eight European countries (22). This contact data exhibits frequent mixing between similar age groups, moderate mixing between children and adults in their thirties (likely their parents), and infrequent mixing between other groups. To generate the contact matrix used in our model, we used the means of each age group over the eight countries. To ensure the matrix is symmetric and convert between age groups used in the survey to those used in our study, we adjusted the contact matrix according to the means for reciprocal age group pairings, following Medlock and Galvani (23). Although US participants were not explicitly included in this survey (22), there was low variability between the eight European countries, and similar mixing patterns recently observed in Japan (24).

To account for behavior change with disease progression in adults, we used primary individual-level data (aggregated data was previously presented in (9)), in which 35 volunteers were experimentally infected with RSV in the US. Severity of RSV symptoms was measured twice daily for two weeks. For each of these days, we considered that an individual withdrew from social activity if the individual reported that at least one of the symptoms “stop me from participating in activities”. Thus, we calculated the daily probability that an individual will withdraw from social interactions $\psi_j(\tau)$ by dividing the number of subjects who changed their behavior by the total number of symptomatic subjects for each day. This procedure yielded an estimate that an RSV infection led to behavior change for an average of 1.1 days in adults. We smoothed the data using a low pass filter Kernel, and scaled the results to ensure that the average number of days of social withdrawal per RSV episode remained 1.1. These patterns of daily behavior and viral load used in our analysis were also consistent with results from another study that followed 85 individuals infected with RSV throughout their infection period (25, 26). For children five years and under, we took into account that an RSV infection has been found to result in 2.3 days of missed daycare (27). We assumed that the timing of these days of withdrawal from social mixing followed the same profile across days as in adults, consistent with the observation that viral load is correlated with severity of symptoms in both children (28) and adults (9, 25).

We estimated the viral load from two clinical studies of the course of RSV infections in young children and adults (25, 28). Both studies used the same methods of nasal wash collection and viral culture with HEp-2 cells to determine the infectious viral load (29). We parameterized the daily viral load in first infections from a clinical study that examined 23 hospitalized infants and toddlers until viral shedding ceased, ten of whom were followed daily (28). The ages of the children ranged from ten days to two years, with a median age of four months, so that it is likely that the measured RSV infection was their first. The average duration of shedding was reported to be 6.7 days. Although not all 23 patients had data reported on a daily basis, a total of 119 daily samples were collected. Using this highly detailed data, we determined the number of days each of the 23 patients had a measurable viral load with an error that is at most 1.1 days. Based on a systematic review of observational and experimental studies in young children and adults infected with RSV (30), as well as similar clinical observations in adults (9, 25, 26), we assumed that there was no measurable viral load for the first two days following exposure and that if infection lead to hospitalization, the first day of hospitalization corresponded to the fifth day of infection. For the viral load data on adults, we converted the data from $\log_{10}(\text{TCID}/\text{mL})$ to $\log_{10}(\text{PFU}/\text{mL})$, and evaluated the mean daily viral load by smoothing the data using a low pass filter Kernel (Fig. S2).

To quantify the daily viral load in symptomatic and asymptomatic subsequent infections, $V_{k=2}(\tau)$ and $V_a(\tau)$, we used primary data from 35 healthy adults who volunteered to be experimentally infected with RSV in the US (aggregated data were previously reported (9)). Severity of symptoms and viral load were

measured twice daily for two weeks. Among these subjects, at least 19 were symptomatic, and 16 experienced very mild to asymptomatic infection (i.e. reported a “just noticeable symptom” or not experiencing “any symptom” (25). We evaluated the daily viral load for the two groups in the same way as for the first infection (Fig. S2 B–C). Our analysis of this primary data demonstrates that mild or asymptomatic infections are associated with lower viral loads than symptomatic infections. Following evidence from a study on adult RSV infection (12), we assumed that 16% of the subsequent infections in individuals five years or under were asymptomatic.

A replicating vaccine may reduce the viral load within the mucosal secretions of a vaccinated individual who became infected (31), thereby also reducing transmission. In our base case, we assumed that vaccination would reduce susceptibility, but not the viral load for those infected. We also conducted a sensitivity analysis of this assumption, where we considered a reduction in viral load of up to 50% for the individuals vaccinated in that season prior to infection versus those unvaccinated in that season prior to infection. All other the fixed parameters used in the transmission model are presented in Table S2.

Table S1. Age-specific contact rates between an infected individual e and their contact j , $C_{e,j}$, based on (22) and adjusted for age distribution (23).

$C_{e,j}$	0–5 months	6–11 months	1 year	2–4 years	5–24 years	25–49 years	50–64 years	≥65 years
0–5 months	43.3	43.3	43.3	43.3	17.7	10.7	6.0	3.8
6–11 months	43.3	43.3	43.3	43.3	17.7	10.7	6.0	3.8
1 year	43.3	43.3	43.3	43.3	17.7	10.7	6.0	3.8
2–4 years	43.3	43.3	43.3	43.3	17.7	10.7	6.0	3.8
5–24 years	17.7	17.7	17.7	17.7	37.1	10.5	8.9	3.9
25–49 years	10.7	10.7	10.7	10.7	10.5	24.0	14.1	6.0
50–64 years	6.0	6.0	6.0	6.0	8.9	14.1	17.7	8.1
≥65 years	3.8	3.8	3.8	3.8	3.9	6.0	8.1	12.3

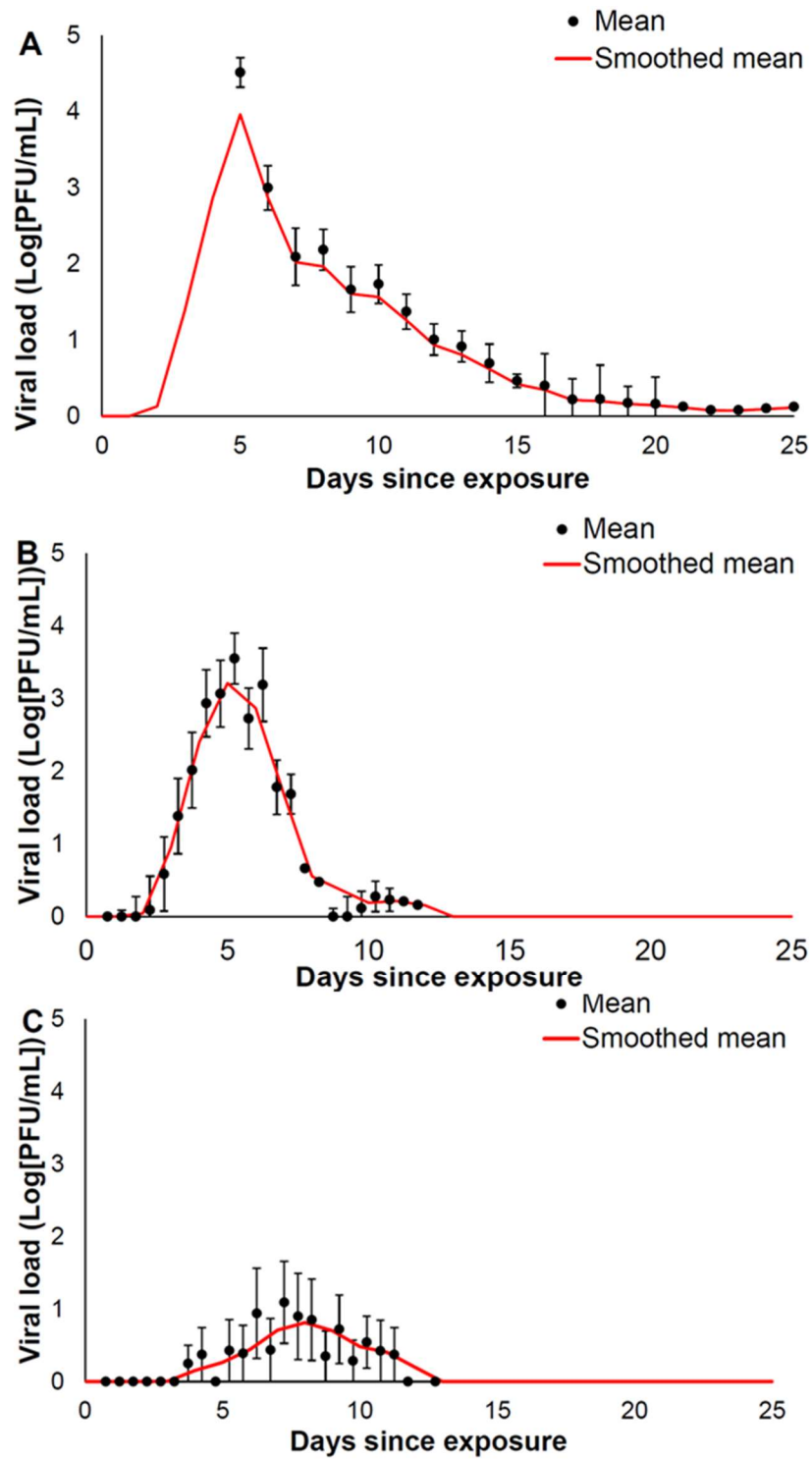


Fig. S2. Daily viral load following RSV infection. Data displayed are the mean (\pm standard error) of the daily viral load. A low pass smoothing curve (red) for (A) the first infection, for (B) symptomatic subsequent infections, and for (C) asymptomatic infection was used to parameterize the viral load progression in the model.

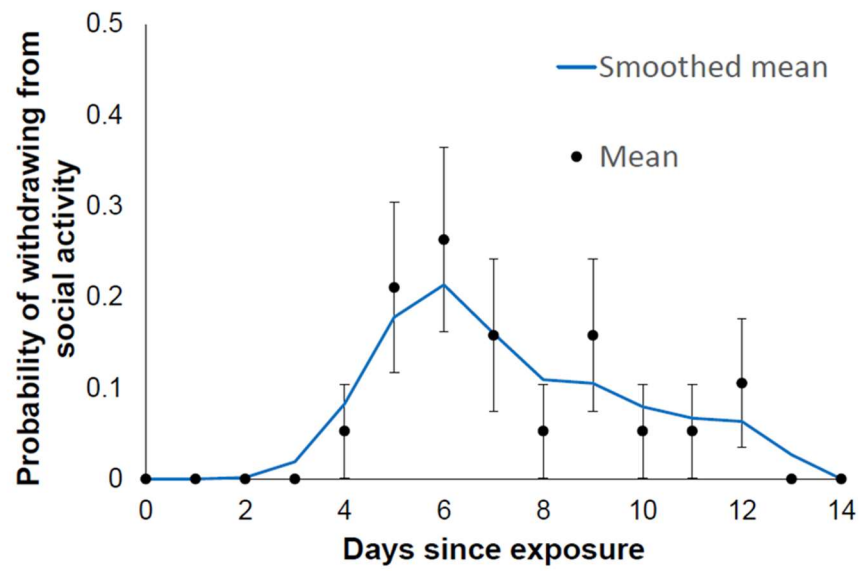


Fig. S3. Effects of RSV on social activity in adults. Data displayed are the mean (\pm standard error) of the daily probability of withdrawal from social activity (25). A low pass smoothing curve (blue) was used to parameterize probability of withdrawal from social activity in the model.

Table S2: Fixed parameters used in the transmission model

Parameter	Description	Value	Justification
Transition Parameters			
$1/w_M$	Average length of maternal immunity	106 days	(3)
$1/w_R$	Average length of recovered immunity	203 days	(4)
α_j	Probability a subsequent infection is asymptomatic	For $j \leq 4$, 0 For $j \geq 5$, 0.16	(10)
Force of Infection			
$\phi_{k=1}$	Length of first infection	26 days	(28)
$\phi_{k=2}$	Length of subsequent infection	13 days	(9)
$\log[V_{k=1}(\tau)]$	Logarithm of viral load on day τ during first infection	Varies	(28)
$\log[V_{k=2}(\tau)]$	Logarithm of viral load on day τ during subsequent symptomatic infection	Varies	(9)
$\log[V_a(\tau)]$	Logarithm of viral load on day τ during subsequent asymptomatic infection	Varies	(9, 27)
$\psi_e(\tau)$	Probability of social withdrawal on day τ for age group e	Varies	(9, 27)
$C_{e,j}$	Contact Matrix for susceptible individual in age group j and infected individual in age-group e	Table S1	(22)
Vaccination Parameters			
v_j	Vaccine efficacy for age group j	40–80%	Broad range tested comparable values with influenza (32)
$p_j(t)$	Rate of vaccination coverage on day t for age group j	Varies	(33)

2.2 Calibrated parameters

Case definition

To estimate empirically unknown epidemiological parameters, we calibrated our model to weekly cases of RSV confirmed by viral isolation, antigen detection or RT PCR between 2010-2014 (34) (Table S3). This data was collected by National Respiratory and Enteric Virus Surveillance System (NREVSS) by the Centers for Disease Control and Prevention (CDC) and state health departments in California, Texas, Pennsylvania, and Colorado.

For children under 5 years, we used a prospective cohort study from Texas to scale the following age-specific incidences of RSV: 0–5, 6–11 months, 1, 2, 3, and 4 years of age (8). No prospective studies estimating rates of RSV in children are available in Pennsylvania, Colorado or California. However, given that in the RSV season, 20–41% of the ILI cases are attributed to RSV infection in children below five (35), we utilize ILI data in 2010-2014 to evaluate RSV rates in these states. Specifically, we calculated the ratios between the ILI rates observed during the RSV seasons in children (stratified by ages 0-5, 6–11 months, 1, 2, 3, and 4) in each of the three states, and the ILI rates observed during the RSV season for the same age group in Texas. The state-specific RSV rates used in the calibration of our model were calculated as a product between these quotients and the RSV rates observed in the prospective cohort study from Texas (8). This evaluation yielded an annual attack rate in children ranging between 30.1% and 62.7%. Regardless of this high variability, our main results are robust: children under five years were responsible for the majority of transmission, and that vaccinating this age group is the most efficient and effective strategy to reduce RSV in both the children as well as adults.

For individuals over five years of age, we used a prospective cohort study in adults to scale incidence of RSV in all four states. Due to the uncertainty related to the actual incidence in adults, we calibrated our model parameters for two settings in each state that correspond to the lowest and highest attack rates, respectively, of RSV seasons observed in adults over five RSV seasons (36). Additionally, following evidence from a study on adult RSV infection (12), we assumed that 16% of the subsequent infections in all individuals over five years were asymptomatic, an assumption which was conservative to our main finding. These evaluations yielded an annual attack rate in individuals over five years ranging between 3.2%, which we considered in our base case and up to 8.3% presented as an alternative analysis of high transmission setting (Fig. S9 and S10).

Calibration

To calibrate the model to the incidence data (Figure S4 and Figure S5) we minimized the squared error between model predictions and incidence data. This is equivalent to maximum likelihood estimation assuming a normal distribution of the error. We conducted this calibration for eight scenarios: to fit model parameters specific to each of the four US states, as well as for both high and base case transmission settings (Table S2) using a simulated annealing minimization algorithm, performing 5,000 iterations per scenario. From biological perspective, we assumed the transmission coefficient (r) should not vary geographically. Because we used data from a prospective study on RSV in children in Texas (8), we were especially confident that the attack rates for Texas were accurate. Thus, we first calibrated our model to data from Texas to estimate r which was also used for the other states. Then, we calibrated the six remaining parameters for Colorado, Pennsylvania and California.

To determine whether we could further reduce the number of free parameters, we evaluated two other model structures, both with six parameters. In the first model structure, we aggregated the parameters reflecting the susceptibility rate of age groups <2 and 2–4. In the second model structure, we aggregated the parameters reflecting the susceptibility rate of age groups 5–49 and ≥ 50 . The reason for evaluating these aggregations was that the weekly incidence of the two age groups composing each of these pairings of age

groups were more similar to each other than were the weekly incidences of other pairings of age groups. To rigorously conduct this comparison of model structure, we calibrated parameters estimated for each model structure and calculated the Akaike Information Criterion (AIC, an information-based criterion for decisions regarding parameter reduction) in Colorado, Pennsylvania, California, and Texas. We found that our seven-parameter model yielded a lower AIC than either six-parameter model structure (Table S1). Because the AIC penalizes for additional parameters less strongly than does the most common alternative information-based criterion (the Bayesian information criterion or BIC; see(37)), we also calculated the BIC for each model structure (Table S1). The BIC likewise yielded a lower score for the seven-parameter model structure, so the criterion used to determine the appropriate model structure does not affect model structure selected. The transmission model that minimizes both the AIC and BIC included seven parameters without constraints imposed from previous data: seasonal offset ϕ , seasonal amplitude A , transmission coefficient r , susceptibility rates for subsequent infection σ_j , for individuals in age groups <2 , $2-4$, $5-49$, and ≥ 50 years of age.

Table S3. Maximum likelihood parameter estimates

Parameter	Seasonal offset	Seasonal amplitude	Transmissibility coefficient	Susceptibility in subsequent infection among <2 years	Susceptibility in subsequent infection among $2-4$ years	Susceptibility in subsequent infection among $5-49$ years	Susceptibility in subsequent infection among ≥ 50 years
Symbol	ϕ	I	r	σ_1	σ_2	σ_3	σ_4
Base case analysis							
California	0.271	0.075	1.22	3.940	0.531	0.088	0.250
Texas	0.170	0.098	1.22	3.142	0.521	0.054	0.130
Pennsylvania	0.606	0.119	1.22	3.074	0.619	0.050	0.120
Colorado	0.125	0.081	1.22	3.331	1.053	0.072	0.169
Alternative analysis of high transmission setting							
California	0.189	0.061	1.22	3.335	0.550	0.214	0.400
Texas	0.984	0.105	1.22	2.780	0.323	0.091	0.163
Pennsylvania	0.732	0.121	1.22	1.620	0.363	0.111	0.181
Colorado	0.111	0.095	1.22	3.359	0.302	0.117	0.212

Table S4**Akaike Information Criterion (AIC)**

State	Scenario	7 parameters	6 parameters ($\sigma_3 = \sigma_4$)	6 parameters ($\sigma_1 = \sigma_2$)
Texas	Base Case	-15186	-14782	-14126
California		-17624	-17411	-17645
Pennsylvania		-15770	-15381	-15098
Colorado		-16876	-16850	-16752
Texas	Alternative Case	-13449	-13275	-13134
California		-15661	-15408	-15920
Pennsylvania		-14131	-13789	-13769
Colorado		-15524	-15441	-15500

Bayesian Information Criterion (BIC)

State	Scenario	7 parameters	6 parameters ($\sigma_3 = \sigma_4$)	6 parameters ($\sigma_1 = \sigma_2$)
Texas	Base Case	-15150	-14751	-14096
California		-17588	-17380	-17614
Pennsylvania		-15735	-15350	-15068
Colorado		-16841	-16819	-16721
Texas	Alternative Case	-13413	-13244	-13103
California		-15625	-15377	-15890
Pennsylvania		-14095	-13758	-13739
Colorado		-15488	-15410	-15469

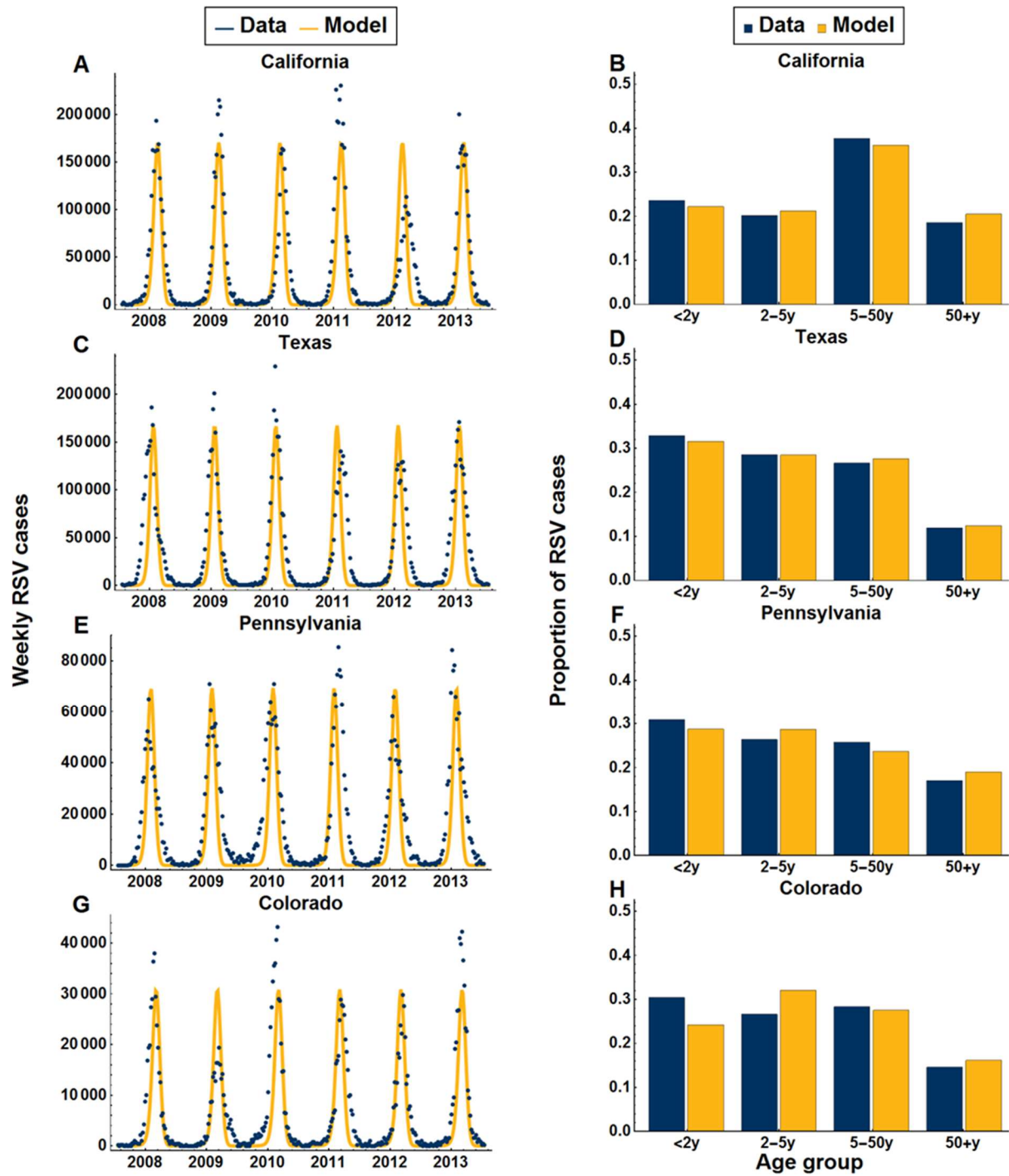


Fig. S4. Base case model fit. Time series of recorded weekly RSV cases and model fit to California, Texas, Colorado, and Pennsylvania (A, C, E, & G). Data and model fit of the age distribution among RSV infections (B, D, F, & H).

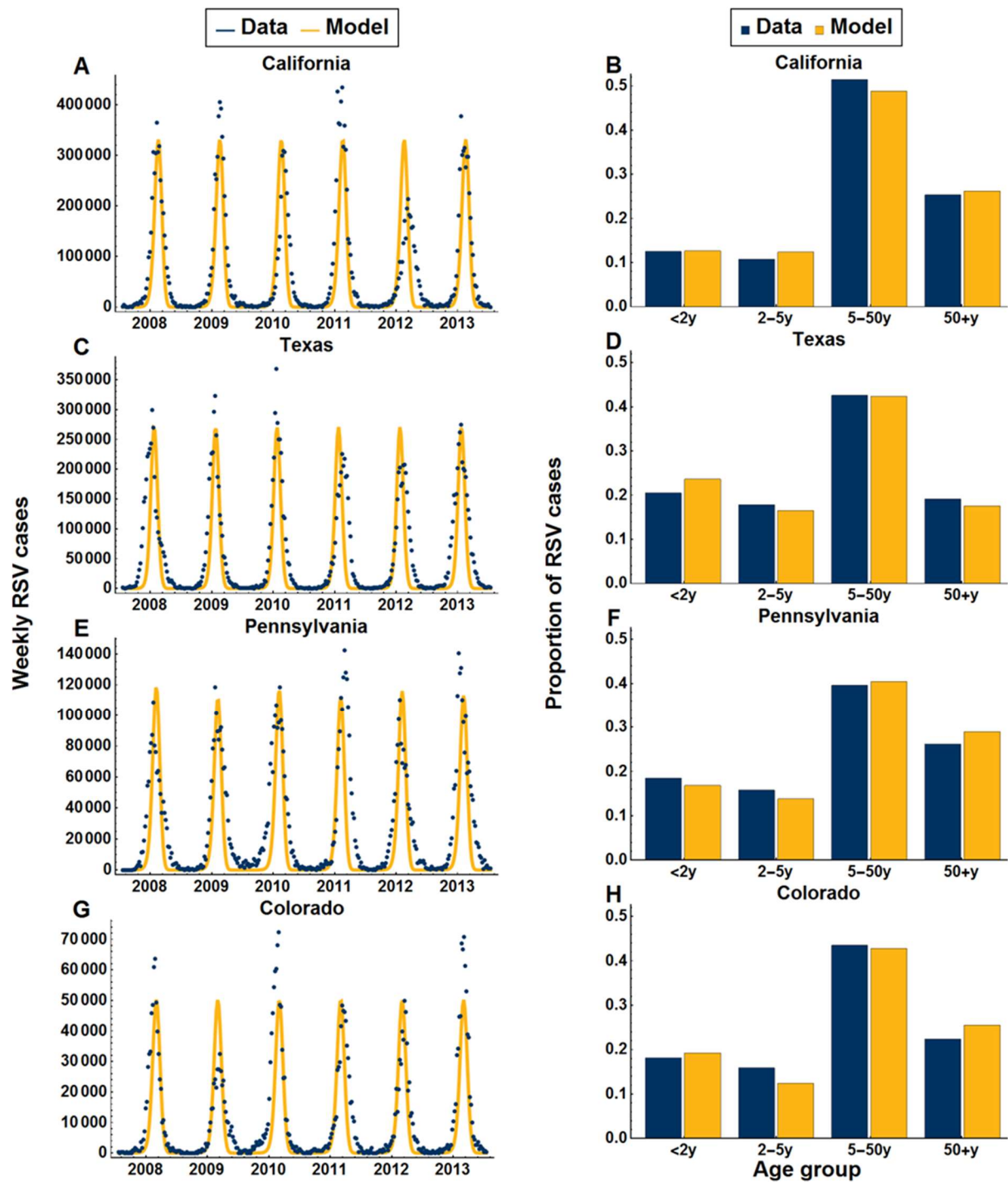


Fig. S5. Alternative model fit of high transmission setting in adults. Time series of recorded weekly RSV cases and model fit to California, Texas, Colorado, and Pennsylvania (A, C, E, & G). Data and model fit of the age distribution among RSV infections (B, D, F, & H).

3. Calculation of secondary cases generated per infection

We calculated the average number of secondary cases generated per infected individual in each age group by evaluating the total number of new cases for which members of an age group had been the source of infection, divided by the total number of infected individuals in that age group (38, 39). Specifically, we simulated an entire RSV seasons in each US state. Throughout the season, we calculated the daily probability that an individual within age-group e , and day of infection τ , would be the source of transmission to individuals from age group j . The probability of infection was calculated as a function of three data-driven factors, which evolve during the progression of infection: 1) the infectious viral load, 2) the probability of withdrawal from social activity, and 3) the expected number of contacts between the age group of the host, n , and the age group of the contact j .

The normalized probability to transmit from an infected individual with infection of type k , in age group e , on day of infection τ , to an individual in age group j was:

$$P_{k,j,e,\tau}(t) = \frac{(r^{\log[V_k(\tau)+1]} - 1) \cdot (C_{e,j}(t)(1 - \psi_j(\tau)) \mathbb{I}_{e,j}) \cdot i_{k,e}^\tau(t-1)}{\sum_{e=1}^n \sum_{k=1}^2 \sum_{\tau=0}^{\varphi_k} (r^{\log[V_k(\tau)+1]} - 1) (C_{e,j}(t)(1 - \psi_j(\tau)) \mathbb{I}_{e,j}) \cdot i_{k,e}^\tau(t-1) + \sum_{e=1}^n \sum_{\tau=0}^{\varphi_k} (r^{\log[V_a(\tau)+1]} - 1) C_{e,j}(t) \cdot a_e^\tau(t-1)}. \quad (11)$$

For asymptomatic infections, this probability of transmission is given by:

$$P_{j,e,\tau}^A(t) = \frac{(r^{\log[V_a(\tau)+1]} - 1) C_{e,j}(t) \cdot a_e^\tau(t-1)}{\sum_{e=1}^n \sum_{k=1}^2 \sum_{\tau=0}^{\varphi_k} (r^{\log[V_k(\tau)+1]} - 1) (C_{e,j}(t)(1 - \psi_j(\tau)) \mathbb{I}_{e,j}) \cdot i_{k,e}^\tau(t-1) + \sum_{e=1}^n \sum_{\tau=0}^{\varphi_k} (r^{\log[V_a(\tau)+1]} - 1) C_{e,j}(t) \cdot a_e^\tau(t-1)}. \quad (12)$$

The number of transmission events $g^\tau(t)$ that occurred on each day of infection, τ , was calculated as a sum of the probabilities of transmission for all infected individuals on calendar date t to yield:

$$g^\tau(t) = \sum_j \sum_e [\sum_{k=1}^2 P_{k,j,e,\tau}(t) \cdot i_{k,j}^0(t) + P_{j,e,\tau}^A(t) \cdot a_j^0(t)]. \quad (13)$$

These results were averaged over the RSV season (or over the first month of the RSV season, depending on the scenario examined), and weighted based on the proportion of the population that was infected on day t :

$$\bar{g}^\tau = \sum_t g^\tau(t) \cdot \frac{\sum_{j=1}^8 [\sum_{k=1}^2 i_{k,j}^0(t) + a_j^0(t)]}{\sum_t \sum_{j=1}^8 [\sum_{k=1}^2 i_{k,j}^0(t) + a_j^0(t)]}. \quad (14)$$

This weighted average, \bar{g}^τ , represents the average number of secondary cases per day of infection (Fig. S7). To evaluate the age-specific average number of secondary infections generated per case (Fig S6 and Fig. 2, Main Text), we considered five age groups: <5 years of age ($e = \{1,2,3,4\}$), 5-24 ($e = \{5\}$), 25-49 ($e = \{6\}$), and ≥ 50 ($e = \{7,8\}$). In Eq. (13), we summed the daily infections over the entire infectious period, φ_k , for each age group.

4. Additional results

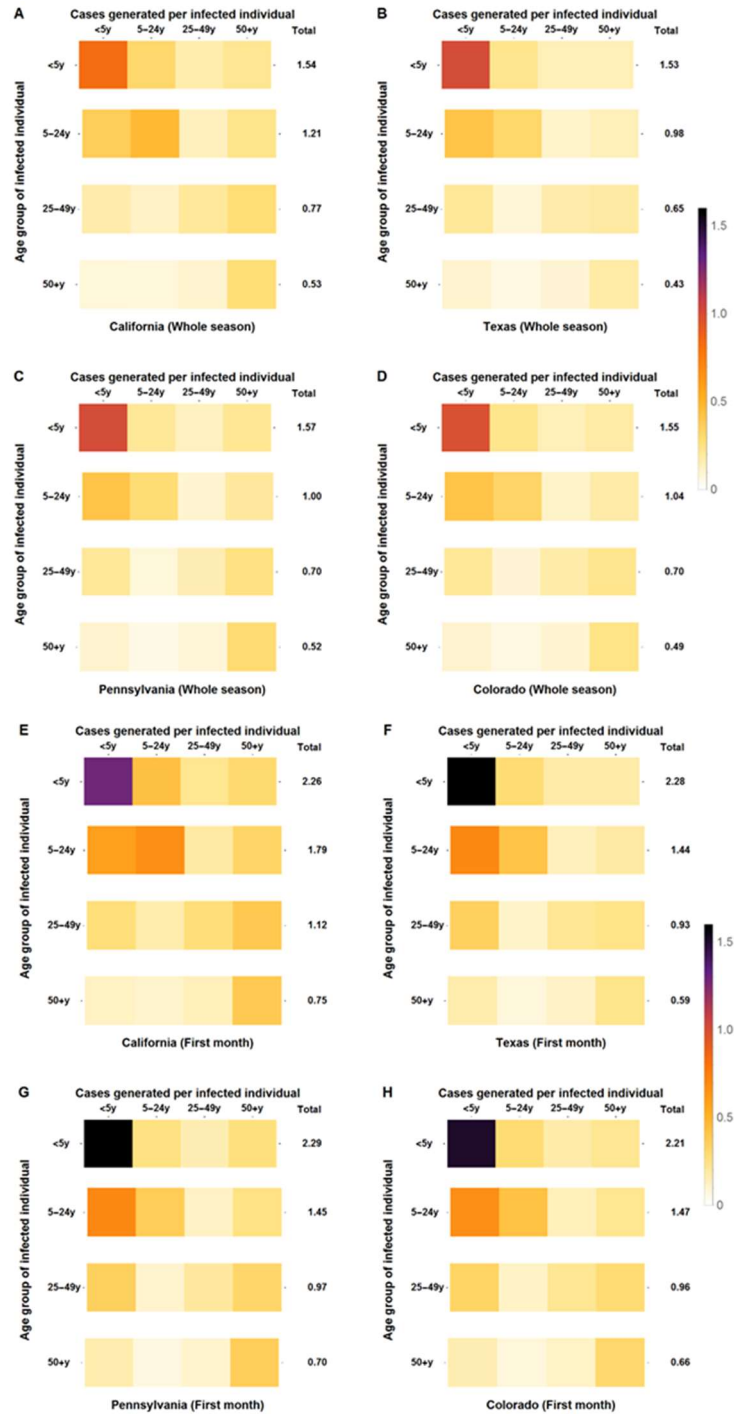


Fig. S6. Age-specific average number of secondary infections generated per case for California (A & E) and Texas (B & F), Pennsylvania (C & G) and Colorado (D & H). Each row identifies an age group that can be a source of infection. Each column identifies an age group that can be infected. The color at the intersection of the row and column indicates the number of secondary infections attributed to a single infective case. The average number of secondary cases from the source age group is tabulated in the

rightmost column of each panel. Model predictions are shown for the entire RSV season (A, B, C & D) and for the first month of the season (E, F, G & H).

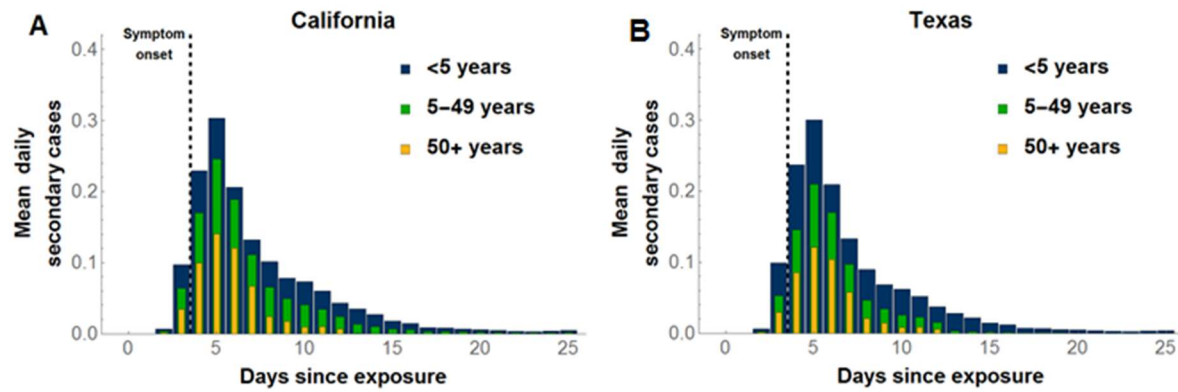


Fig. S7. Age-stratified mean daily number of secondary cases in (A) California, (B) Texas. Similar trends have been observed in Pennsylvania, and Colorado.

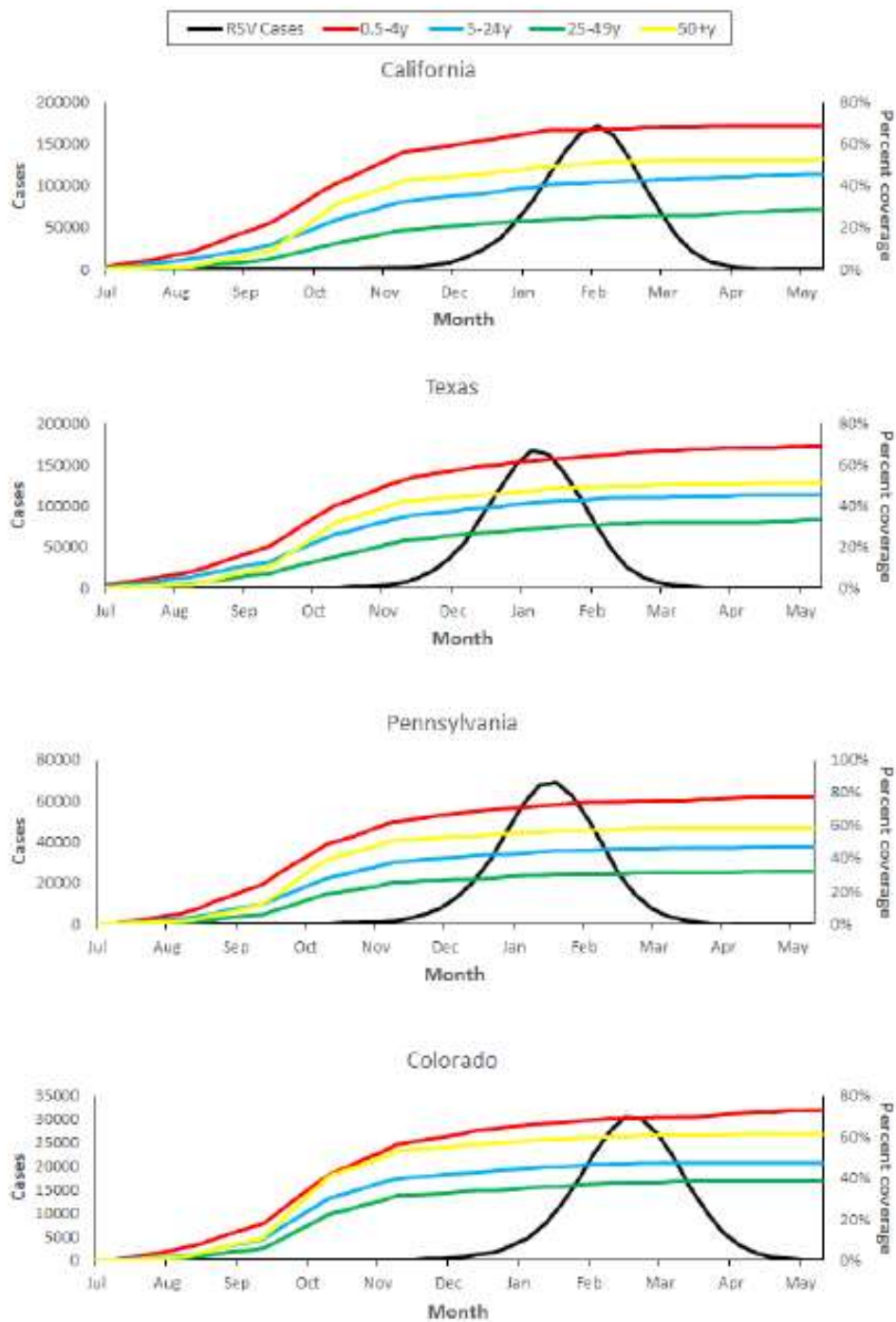


Fig. S8. State-specific cumulative vaccination coverage stratified by age throughout the RSV season. We assumed that RSV vaccination uptake is the same monthly coverage observed for influenza between 2010 and 2014 given plans to administer the RSV vaccine together. RSV peaks first in Texas, Pennsylvania, California and Colorado.

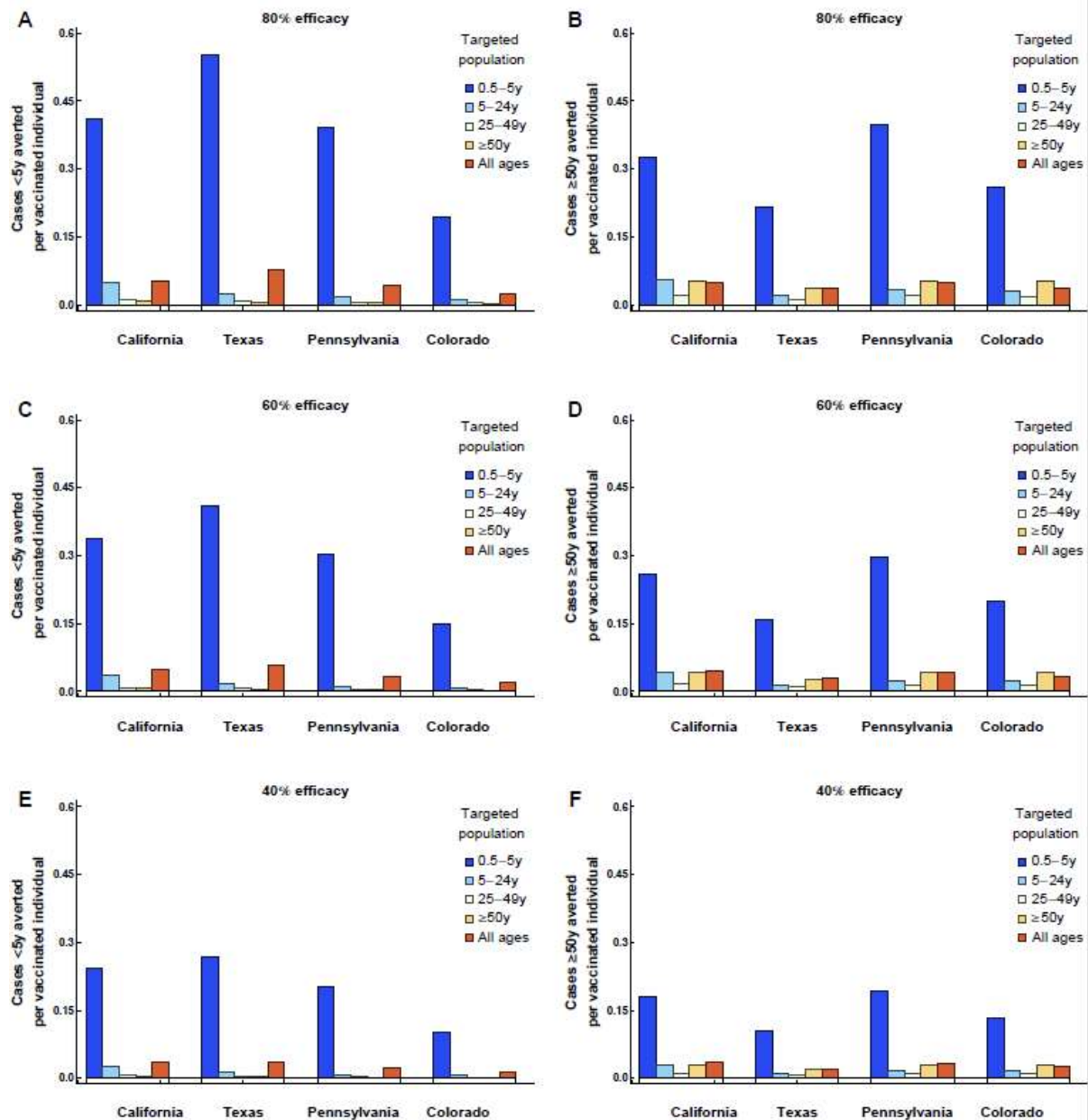


Fig. S9. Per-dose vaccine efficiency in alternative model setting of high transmission in adults. Model predictions of RSV cases averted per vaccinated individual in California, Texas, Pennsylvania, and Colorado, assuming a vaccination efficacy of 80% (A & B), 60% (C & D), and 40% (E & F). Here, no reduction in viral load is assumed for vaccinated individuals who became infected. Cases averted are tallied for the two at-risk age groups: individuals below five years (A, C & E), and individuals fifty years and above (B, D & F).

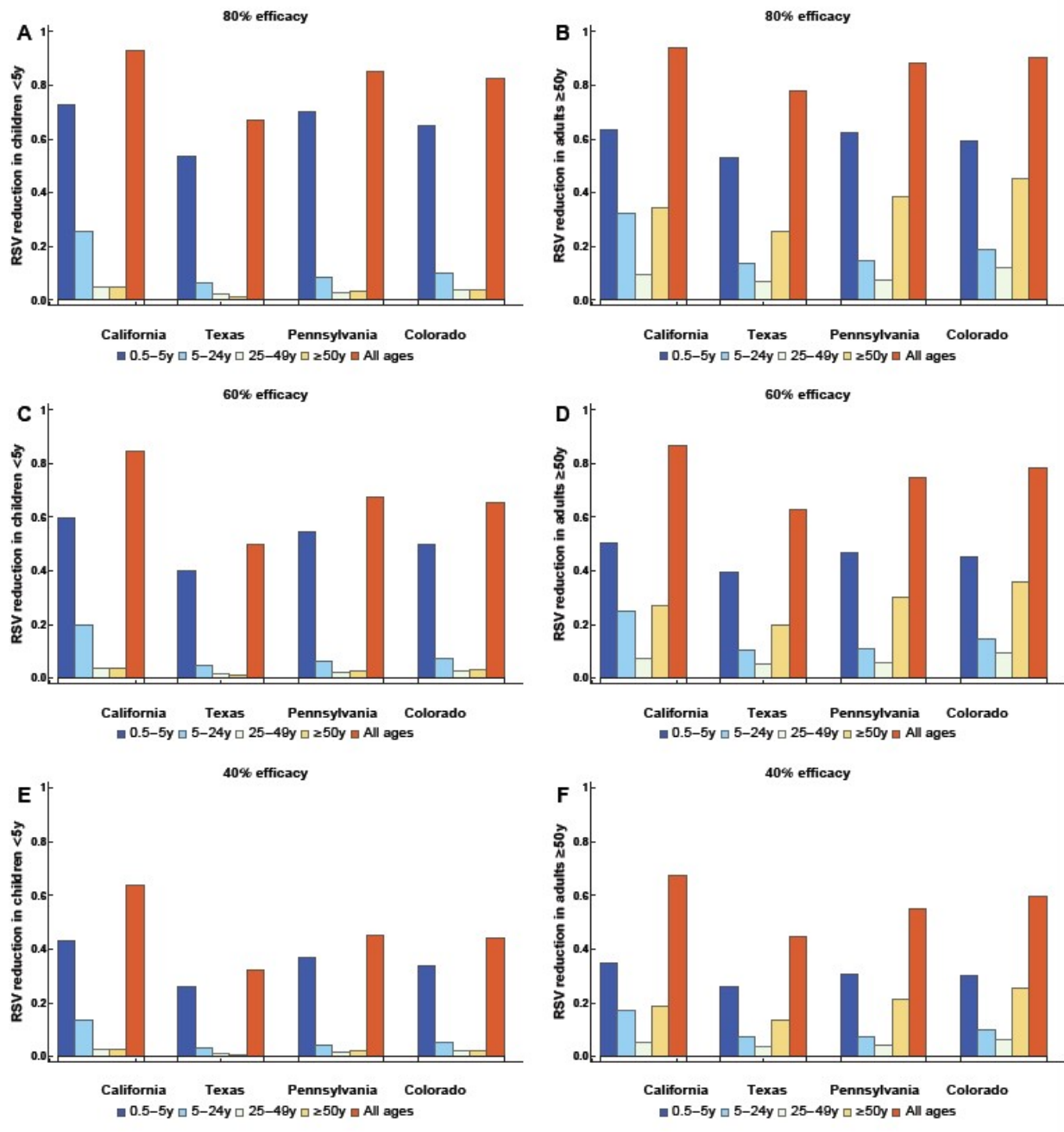


Fig. S10. Model projections of proportion reduction in RSV cases for alternative model setting of high transmission in adults in California, Texas, Pennsylvania, and Colorado, assuming vaccination efficacy of 80% (A & B), 60% (C & D), and 40% (E & F). Here, no reduction in viral load was imposed on vaccinated individuals who became infected. Cases averted are tallied for the two at-risk age groups: individuals below five years (A, C & E), and individuals fifty years and above (B, D & F).

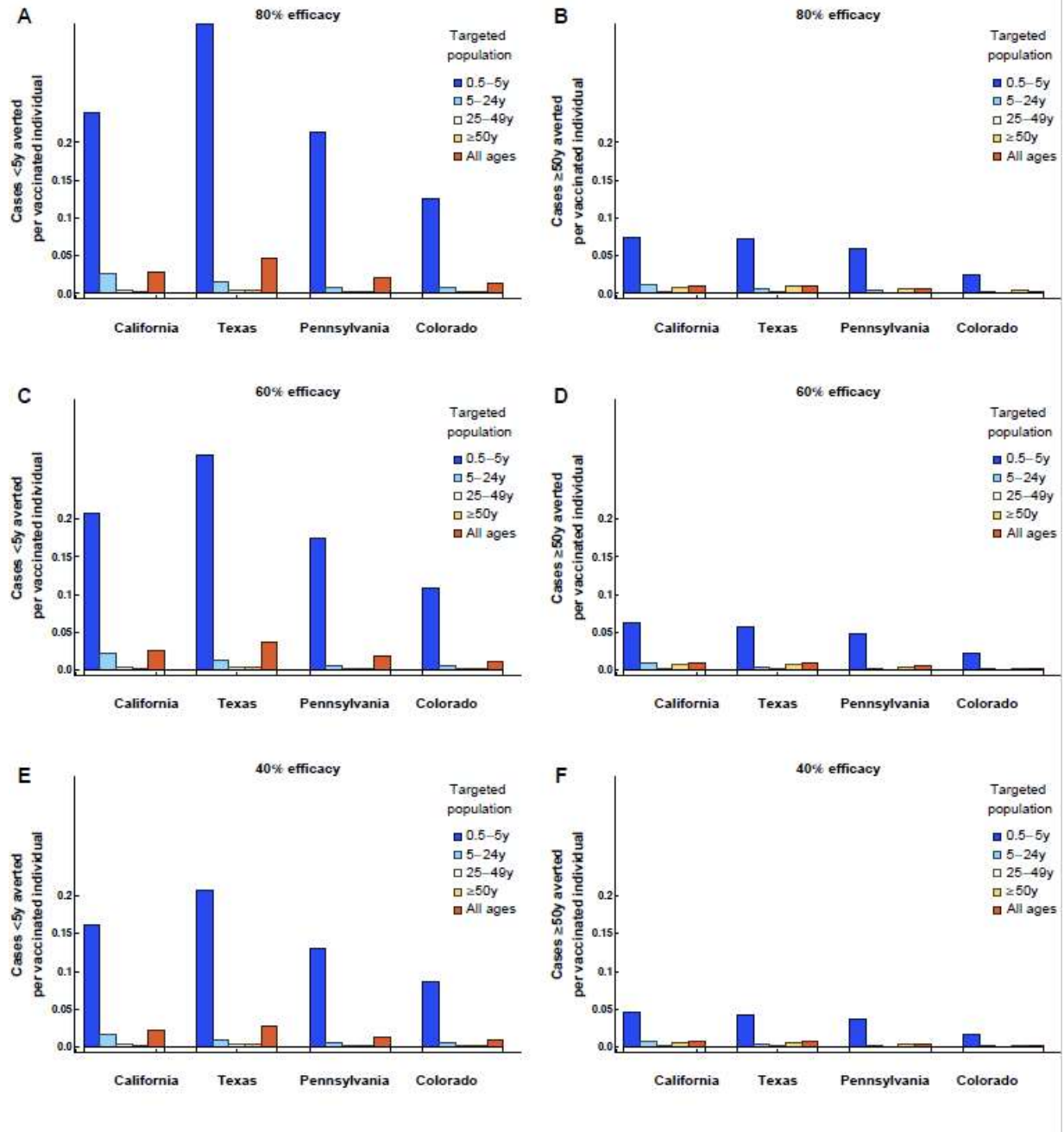


Fig. S11. Model predictions of RSV cases averted per vaccinated individual in California, Texas, Pennsylvania, and Colorado, assuming vaccine efficacies of 80% (A & B), 60% (C & D), and 40% (E & F). Here, 50% reduction in viral load is assumed for vaccinated individuals who became infected during the same RSV season. Cases averted are tallied for the two at-risk age groups: individuals below five years (A, C & E), and individuals fifty years and above (B, D & F).

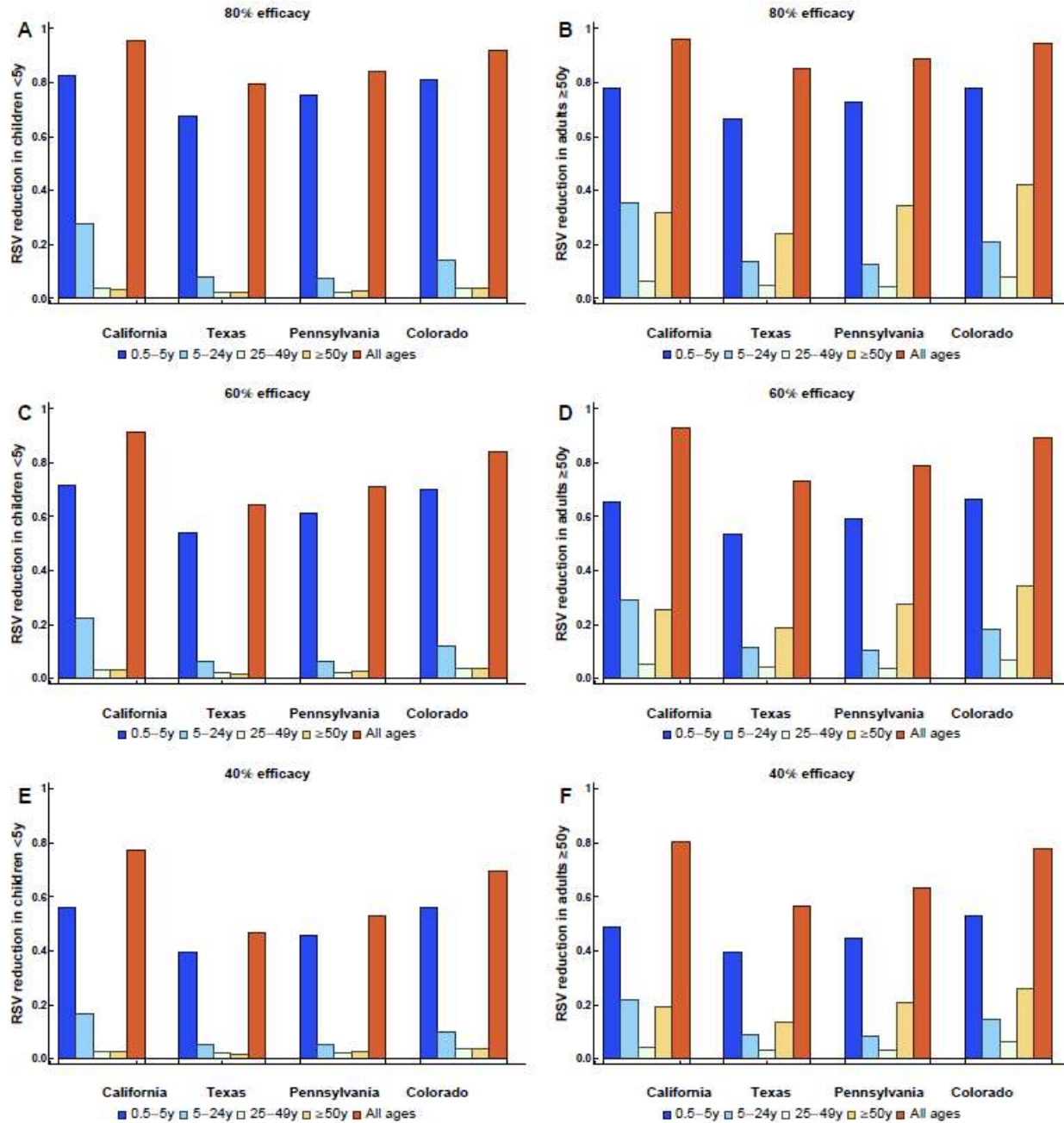


Fig. S12. Model predictions of proportion reduction in RSV cases in California, Texas, Pennsylvania, and Colorado, assuming vaccine efficacies of 80% (A & B), 60% (C & D), and 40% (E & F). Here, 50% reduction in viral load was assumed for vaccinated individuals who became infected during the same RSV season. Cases averted are tallied for the two at-risk age groups: individuals below five years (A, C & E), and individuals fifty years and above (B, D & F)

5. Model and simulation analysis code in Mathematica 10

```

runModel[phi_, F_, r_, sigmaBaby_, sigmaChild_, sigmaAdult_, sigmaOld_] := Module[
  {lambda, i, va, vi, a, eqS, eqM, sigma, eqP, eqI, eqA, expr,
   eqns, initcon, out, t, eqR, eqVS, eqVI, eqVA, eqVR, eqVM},

  (*sigmas*)
  Table[sigma_j = sigmaBaby, {j, 1, 3}];
  Table[sigma_j = sigmaChild, {j, 4, 4}];
  Table[sigma_j = sigmaAdult, {j, 5, 6}];
  Table[sigma_j = sigmaOld, {j, 7, agegroup}];

  Table[lambda_j = Max[0, (F + F * Cos[2 * N[pi] * (t - phi) / 365.242]) *
    (Sum[w=0 to tau1-1 Sum[h=1 to agegroup (ContactI[[w+1, j, h]] * (eqI1,h,w[t-1] * (r^(v1[[w+1]])) - 1) +
      eqVI1,h,w[t-1] * (r^(gamma * v1[[w+1]])) - 1)) +
    Sum[y=0 to tau2-1 Sum[h=1 to agegroup (ContactI[[y+1, j, h]] * (eqI2,h,y[t-1] *
      (r^(v2[[y+1]])) - 1) + eqVI2,h,y[t-1] * (r^(gamma * v2[[y+1]])) - 1) +
    ContactA[[j, h]] * (eqA_h,y[t-1] * (r^(vA[[y+1]])) - 1) +
    eqVA_h,y[t-1] * (r^(gamma * vA[[y+1]])) - 1)))]],
    {j, 1, 8}];

  eqns = Flatten[{
    Table[eqM_j[t] == eqM_j[t-1] + lambda_j / eta + d_{j-1} * eqM_{j-1}[t-1] -
      (d_j + mu_j + omega_M + chi_j[t-1]) * eqM_j[t-1] + omega_V[t-1] * eqVM_j[t-1], {j, 1, 8}],
    Table[eqS1,j[t] == eqS1,j[t-1] + d_{j-1} * eqS1,j-1[t-1] - (d_j + mu_j + lambda_j + chi_j[t-1]) *
      eqS1,j[t-1] + omega_M * eqM_j[t-1] + omega_V[t-1] * eqVS1,j[t-1], {j, 1, 8}],
    Table[eqS2,j[t] == eqS2,j[t-1] + d_{j-1} * eqS2,j-1[t-1] - (d_j + mu_j + sigma_j * lambda_j + chi_j[t-1]) *
      eqS2,j[t-1] + omega_R * eqR_j[t-1] + omega_V[t-1] * eqVS2,j[t-1] - 1 / 8 / eta, {j, 1, 8}],
    Table[eqI1,j,0[t] == lambda_j * eqS1,j[t-1] + 1 / (2 * 8) / eta, {j, 1, agegroup}],
    Table[eqI1,j,m[t] == (1 - mu_j - d_j) * eqI1,j,m-1[t-1] + d_{j-1} * eqI1,j-1,m-1[t-1],
      {j, 1, agegroup}, {m, 1, tau1 - 1}],
    Table[eqI2,j,0[t] ==
      lambda_j * sigma_j * (1 - alpha[[j]]) * eqS2,j[t-1] + 1 / (2 * 8) / eta, {j, 1, agegroup}],
    Table[eqI2,j,m[t] == (1 - mu_j - d_j) * eqI2,j,m-1[t-1] + d_{j-1} * eqI2,j-1,m-1[t-1],
      {j, 1, agegroup}, {m, 1, tau2 - 1}],
  ]

```

Table[eqA_{j,0}[t] == λ_j * σ_j * α[[j]] * eqS_{2,j}[t-1], {j, 1, agegroup}],
Table[eqA_{j,m}[t] == (1 - μ_j - d_j) * eqA_{j,m-1}[t-1] + d_{j-1} * eqA_{j-1,m-1}[t-1],
{j, 1, agegroup}, {m, 1, τ₂-1}],

Table[eqR_j[t] ==
eqR_j[t-1] - (d_j + μ_j) * eqR_j[t-1] - ω_R * eqR_j[t-1] + d_{j-1} * eqR_{j-1}[t-1] +
(1 - μ_j - d_j) * (eqI_{1,j,τ₁-1}[t-1] + eqI_{2,j,τ₂-1}[t-1] + eqA_{j,τ₂-1}[t-1]) +
d_{j-1} * (eqI_{1,j-1,τ₁-1}[t-1] + eqI_{2,j-1,τ₂-1}[t-1] + eqA_{j-1,τ₂-1}[t-1]) +
ω_V[t-1] * eqVR_j[t-1], {j, 1, agegroup}],

Table[eqVM_j[t] == eqVM_j[t-1] + d_{j-1} * eqVM_{j-1}[t-1] - (d_j + μ_j + ω_M) * eqVM_j[t-1] +
χ_j[t-1] * (1 - ρ_j) * eqM_j[t-1] - ω_V[t-1] * eqVM_j[t-1], {j, 1, agegroup}],

Table[eqVS_{1,j}[t] == eqVS_{1,j}[t-1] + ω_M * eqVM_j[t-1] +
d_{j-1} * eqVS_{1,j-1}[t-1] + χ_j[t-1] * (1 - ρ_j) * eqS_{1,j}[t-1] -
(d_j + μ_j + ω_V[t-1] + λ_j) * eqVS_{1,j}[t-1], {j, 1, agegroup}],

Table[eqVS_{2,j}[t] ==
eqVS_{2,j}[t-1] + d_{j-1} * eqVS_{2,j-1}[t-1] - (d_j + μ_j + ω_V[t-1] + σ_j * λ_j) * eqVS_{2,j}[t-1] +
χ_j[t-1] * (1 - ρ_j) * eqS_{2,j}[t-1] + ω_R * eqVR_j[t-1], {j, 1, agegroup}],

Table[eqVI_{1,j,0}[t] == λ_j * eqVS_{1,j}[t-1], {j, 1, agegroup}],

Table[eqVI_{1,j,m}[t] == (1 - μ_j - d_j) * eqVI_{1,j,m-1}[t-1] + d_{j-1} * eqVI_{1,j-1,m-1}[t-1],
{j, 1, agegroup}, {m, 1, τ₁-1}],

Table[eqVI_{2,j,0}[t] == (1 - α[[j]]) * σ_j * λ_j * eqVS_{2,j}[t-1], {j, 1, agegroup}],

Table[eqVI_{2,j,m}[t] == (1 - μ_j - d_j) * eqVI_{2,j,m-1}[t-1] + d_{j-1} * eqVI_{2,j-1,m-1}[t-1],
{j, 1, agegroup}, {m, 1, τ₂-1}],

Table[eqVA_{j,0}[t] == α[[j]] * σ_j * λ_j * eqVS_{2,j}[t-1], {j, 1, agegroup}],

Table[eqVA_{j,m}[t] == (1 - μ_j - d_j) * eqVA_{j,m-1}[t-1] + d_{j-1} * eqVA_{j-1,m-1}[t-1],
{j, 1, agegroup}, {m, 1, τ₂-1}],

Table[eqVR_j[t] ==
eqVR_j[t-1] - (d_j + μ_j + ω_V[t-1] + ω_R) * eqVR_j[t-1] + d_{j-1} * eqVR_{j-1}[t-1] +
(1 - μ_j - d_j) * (eqVI_{1,j,τ₁-1}[t-1] + eqVI_{2,j,τ₂-1}[t-1] + eqVA_{j,τ₂-1}[t-1]) +
d_{j-1} * (eqVI_{1,j-1,τ₁-1}[t-1] + eqVI_{2,j-1,τ₂-1}[t-1] + eqVA_{j-1,τ₂-1}[t-1]) +
(χ_j[t-1] * ρ_j) * (eqM_j[t-1] + eqS_{1,j}[t-1] + eqS_{2,j}[t-1]), {j, 1, agegroup}]

}};

initcon = {

```

Table[
  eqMj[0] == {(n01 / η - .0001) / 2, 0, 0, 0, 0, 0, 0, 0, 0}[[j]], {j, 1, agegroup}],
Table[eqS1,j[0] == {(n01 / η - .0001) / 2, n02 / (η) - .0001,
  (n03 / η - .0001) / 2, 0, 0, 0, 0, 0, 0}[[j]], {j, 1, agegroup}],
Table[eqS2,j[0] == {0.00000, 0.00000, (n03 / η - .0001) / 2,
  n04 / (η) - .0001, n05 / (η) - .0001, n06 / (η) - .0001,
  n07 / (η) - .0001, n08 / (η) - .0001}[[j]], {j, 1, agegroup}],
Table[Table[eqI1,j,m[0] == {(0.0001, .0001, 0, 0, 0, 0, 0, 0, 0) / τ1}[[j]],
  {j, 1, agegroup}], {m, 0, τ1 - 1}],
Table[Table[eqI2,j,m[0] == {(0, 0, (1 - α[[j]]) * .0001, (1 - α[[j]]) * .0001,
  (1 - α[[j]]) * .0001, (1 - α[[j]]) * .0001, (1 - α[[j]]) * .0001,
  (1 - α[[j]]) * .0001) / τ2}[[j]], {j, 1, agegroup}], {m, 0, τ2 - 1}],
Table[Table[eqAj,m[0] == {(0, 0, α[[j]] * .0001, α[[j]] * .0001,
  α[[j]] * .0001, α[[j]] * .0001, α[[j]] * .0001, α[[j]] * .0001) / τ2}[[j]],
  {j, 1, agegroup}], {m, 0, τ2 - 1}],
Table[eqRj[0] == {0, 0, 0, 0, 0, 0, 0, 0, 0}[[j]], {j, 1, agegroup}],
Table[eqVS1,j[0] == {0, 0, 0, 0, 0, 0, 0, 0, 0}[[j]], {j, 1, agegroup}],
Table[eqVS2,j[0] == {0, 0, 0, 0, 0, 0, 0, 0, 0}[[j]], {j, 1, agegroup}],
Table[Table[eqVI1,j,m[0] == {(0, 0, 0, 0, 0, 0, 0, 0, 0) / τ1}[[j]],
  {j, 1, agegroup}], {m, 0, τ1 - 1}],
Table[Table[eqVI2,j,m[0] == {(0, 0, 0, 0, 0, 0, 0, 0, 0) / τ2}[[j]],
  {j, 1, agegroup}], {m, 0, τ2 - 1}],
Table[Table[eqVAj,m[0] == {(0, 0, 0, 0, 0, 0, 0, 0, 0) / τ2}[[j]],
  {j, 1, agegroup}], {m, 0, τ2 - 1}],
Table[eqVRj[0] == {0, 0, 0, 0, 0, 0, 0, 0, 0}[[j]], {j, 1, agegroup}],
Table[eqVMj[0] == {0, 0, 0, 0, 0, 0, 0, 0, 0}[[j]], {j, 1, agegroup}]
];

expr = Flatten[Transpose[Table[Flatten[{
  eqMj, eqS1,j, eqS2,j, Table[eqI1,j,m, {m, 0, τ1 - 1}],
  Table[eqI2,j,m, {m, 0, τ2 - 1}], Table[eqAj,m, {m, 0, τ2 - 1}],
  eqRj, eqVS1,j, eqVS2,j, Table[eqVI1,j,m, {m, 0, τ1 - 1}],
  Table[eqVI2,j,m, {m, 0, τ2 - 1}], Table[eqVAj,m, {m, 0, τ2 - 1}], eqVRj, eqVMj
}], {j, 1, agegroup}]]];

out = Transpose[RecurrenceTable[
  Flatten[{eqns, initcon}], expr, {t, 0, Round[years * 365.242]}]]
]

(*Model simulations *)

years = 15; (*How long the model should run for*)
burnInYearsForVacc = 5;
(* note- burning should be similar in the paramter setting as well!!! *)

```



```

 $\gamma = 0.5;$ 
transmission = 0;
While[transmission < 1, {transmission = transmission + 1;
  state = 0;
  Print["wait for a while- transmission"];
  While[ state < 4, { state = state + 1;
    (* 1 = CALIFORNIA, 2 = TEXAS, 3 = PENNSYLVANIA, 4 = COLORADO *)
    (*kids 0-5 *)
    setDemographics[state];
    setVaccRate[state];
    setWane;
    Varate = 0.2;
    Vnum = 0;
    { $\rho_1, \rho_2, \rho_3, \rho_4, \rho_5, \rho_6, \rho_7, \rho_8$ } = {0, 0, 0, 0, 0, 0, 0, 0};
    output = runModel @@ setting[[state]][[transmission]];
    outputForAnalysis = Table[Total[output[[1 ;; -2]]][[
      i, burnInYearsForVacc * 365 + 1 ;; -1]], {i, 1, agegroup}];
    totalinfection[1][1][Vnum][state][transmission] = Total[Table[
      Total[outputForAnalysis[[i]]], {i, 1, 4}]]; (* i- poulation vaccinated,
    j- poulation affected - kids/elderly, k- vaccination scenario *)
    totalinfection[1][2][Vnum][state][transmission] =
      Total[Table[Total[outputForAnalysis[[i]]], {i, 7, 8}]];
    Print["wait for a while state"];

    (* kids *)
    While[ Varate < 0.8, {
      Varate = Varate + 0.1; Vnum = Vnum + 1;
      { $\rho_1, \rho_2, \rho_3, \rho_4, \rho_5, \rho_6, \rho_7, \rho_8$ } = {0, Varate, Varate, Varate, 0, 0, 0, 0};

      Table[ $\chi_j[t - 1] = 0, \{t, 1, stopT - startT + 1\}, \{j, 5, 8\}];

      output = runModel @@ setting[[state]][[transmission]];
      outputForAnalysis = Table[Total[output[[1 ;; -2]]][[
        i, burnInYearsForVacc * 365 + 1 ;; -1]], {i, 1, agegroup}];
      totalinfection[1][1][Vnum][state][transmission] =
        Total[Table[Total[outputForAnalysis[[i]]], {i, 1, 4}]];
      (* i- poulation vaccinated, j- poulation affected - kids/elderly,
      k- vaccination scenario *)
      totalinfection[1][2][Vnum][state][transmission] =
        Total[Table[Total[outputForAnalysis[[i]]], {i, 7, 8}]];
      Print["wait for a while vaccination rate"];}];
    (** end kids vaccinated 0-5*)
    Varate = 0.2;
    Vnum = 0;

    (* Teens *)
    While[ Varate < 0.8, {$ 
```

```

setVaccRate[state];
Table[χj[t-1] = 0, {t, 1, stopT - startT + 1}, {j, 1, 4}];
Table[χj[t-1] = 0, {t, 1, stopT - startT + 1}, {j, 6, 8}];

Varate = Varate + 0.1; Vnum = Vnum + 1;
{ρ1, ρ2, ρ3, ρ4, ρ5, ρ6, ρ7, ρ8} = {0, 0, 0, 0, Varate, 0, 0, 0};
output = runModel@@setting[[state]][[transmission]];
outputForAnalysis = Table[Total[output[[1 ;; -2]]][[
  i, burnInYearsForVacc * 365 + 1 ;; -1]], {i, 1, agegroup}];
totalinfection[2][1][Vnum][state][transmission] =
  Total[Table[Total[outputForAnalysis[[i]]], {i, 1, 4}]];
(* i- poulation vaccinated, j- poulation affected - kids/elderly,
k- vaccination scenario *)
totalinfection[2][2][Vnum][state][transmission] =
  Total[Table[Total[outputForAnalysis[[i]]], {i, 7, 8}]]];];

(* end 5-25 vaccinated *)

Varate = 0.2;
Vnum = 0; (* adults *)
While[ Varate < 0.8, {

  setVaccRate[state];
  Table[χj[t-1] = 0, {t, 1, stopT - startT + 1}, {j, 1, 5}];
  Table[χj[t-1] = 0, {t, 1, stopT - startT + 1}, {j, 7, 8}];

  Varate = Varate + 0.1; Vnum = Vnum + 1;
  {ρ1, ρ2, ρ3, ρ4, ρ5, ρ6, ρ7, ρ8} = {0, 0, 0, 0, 0, Varate, 0, 0};
  output = runModel@@setting[[state]][[transmission]];
  outputForAnalysis = Table[Total[output[[1 ;; -2]]][[
    i, burnInYearsForVacc * 365 + 1 ;; -1]], {i, 1, agegroup}];
  totalinfection[3][1][Vnum][state][transmission] =
    Total[Table[Total[outputForAnalysis[[i]]], {i, 1, 4}]];
  (* i- poulation vaccinated, j- poulation affected - kids/elderly,
  k- vaccination scenario *)
  totalinfection[3][2][Vnum][state][transmission] =
    Total[Table[Total[outputForAnalysis[[i]]], {i, 7, 8}]]];];

Varate = 0.2;
Vnum = 0; (*elderly *)
While[ Varate < 0.8, {

  setVaccRate[state];
  Table[χj[t-1] = 0, {t, 1, stopT - startT + 1}, {j, 1, 6}];

  Varate = Varate + 0.1; Vnum = Vnum + 1;
  {ρ1, ρ2, ρ3, ρ4, ρ5, ρ6, ρ7, ρ8} = {0, 0, 0, 0, 0, 0, Varate, Varate};
  output = runModel@@setting[[state]][[transmission]];

```

```

outputForAnalysis = Table[Total[output[[1 ;; -2]]][[
  i, burnInYearsForVacc * 365 + 1 ;; -1]], {i, 1, agegroup}];
totalinfection[4][1][Vnum][state][transmission] =
  Total[Table[Total[outputForAnalysis[[i]]], {i, 1, 4}]];
(* i- poulation vaccinated, j- poulation affected - kids/elderly,
k- vaccination scenario *)
totalinfection[4][2][Vnum][state][transmission] =
  Total[Table[Total[outputForAnalysis[[i]]], {i, 7, 8}]]];];

Varate = 0.2;
Vnum = 0; (* all *)
While[ Varate < 0.8, {
  setVaccRate[state];
  Varate = Varate + 0.1; Vnum = Vnum + 1;
  { $\rho_1, \rho_2, \rho_3, \rho_4, \rho_5, \rho_6, \rho_7, \rho_8$ } =
    {Varate, Varate, Varate, Varate, Varate, Varate, Varate, Varate};
  output = runModel @@ setting[[state]][[transmission]];
  outputForAnalysis = Table[Total[output[[1 ;; -2]]][[
    i, burnInYearsForVacc * 365 + 1 ;; -1]], {i, 1, agegroup}];
  totalinfection[5][1][Vnum][state][transmission] =
    Total[Table[Total[outputForAnalysis[[i]]], {i, 1, 4}]];
  (* i- poulation vaccinated, j- poulation affected - kids/elderly,
  k- vaccination scenario *)
  totalinfection[5][2][Vnum][state][transmission] =
    Total[Table[Total[outputForAnalysis[[i]]], {i, 7, 8}]]];];
}];]; // Timing

TInew = Table[totalinfection[q][i][w][j][k],
  {q, 1, 5}, {i, 1, 2}, {w, 1, 6}, {j, 1, 4}, {k, 1, 1}];

```

References and notes

1. Vynnycky E, White R (2010) *An Introduction to Infectious Disease Modelling* (Oxford University Press, USA).
2. Ogilvie MM, Vathenen AS, Radford M, Codd J, Key S (1981) Maternal antibody and respiratory syncytial virus infection in infancy. *J Med Virol* 7(4):263–71.
3. Ochola R, et al. (2009) The level and duration of RSV-specific maternal IgG in infants in Kilifi Kenya. *PLoS One* 4(12):e8088.
4. Weber A, Weber M, Milligan P (2001) Modeling epidemics caused by respiratory syncytial virus (RSV). *Math Biosci* 172(2):95–113.
5. WHITE LJ, WARIS M, CANE PA, NOKES DJ, MEDLEY GF (2005) The transmission dynamics of groups A and B human respiratory syncytial virus (hRSV) in England & Wales and Finland: seasonality and cross-protection. *Epidemiol Infect* 133(2):279–289.
6. White LJ, et al. (2007) Understanding the transmission dynamics of respiratory syncytial virus using multiple time series and nested models. *Math Biosci* 209(1):222–39.
7. Pitzer VE, et al. (2015) Environmental drivers of the spatiotemporal dynamics of respiratory syncytial virus in the United States. *PLoS Pathog* 11(1):e1004591.
8. Glezen WP (1986) Risk of Primary Infection and Reinfection With Respiratory Syncytial Virus. *Arch Pediatr Adolesc Med* 140(6):543.
9. DeVincenzo JP, et al. (2010) Viral load drives disease in humans experimentally infected with respiratory syncytial virus. *Am J Respir Crit Care Med* 182(10):1305–14.
10. Hall CB, Long CE, Schnabel KC (2001) Respiratory syncytial virus infections in previously healthy working adults. *Clin Infect Dis* 33(6):792–6.
11. Hall CB, Walsh EE, Long CE, Schnabel KC (1991) Immunity to and frequency of reinfection with respiratory syncytial virus. *J Infect Dis* 163(4):693–8.
12. Hall CB, Long CE, Schnabel KC (2001) Respiratory Syncytial Virus Infections in Previously Healthy Working Adults. 14642:792–796.
13. Panozzo CA, Fowlkes AL, Anderson LJ (2007) Variation in timing of respiratory syncytial virus outbreaks: lessons from national surveillance. *Pediatr Infect Dis J* 26(11 Suppl):S41–5.
14. Funk S, Salathé M, Jansen VAA (2010) Modelling the influence of human behaviour on the spread of infectious diseases: a review. *J R Soc Interface* 7(50):1247–56.
15. Tellier R (2009) Aerosol transmission of influenza A virus: a review of new studies. *J R Soc Interface* 6 Suppl 6:S783–90.
16. Heikkinen T, Valkonen H, Waris M, Ruuskanen O (2015) Transmission of respiratory syncytial virus infection within families. *Open forum Infect Dis* 2(1):ofu118.
17. Couch RB, Knight V, Douglas RG, Black SH, Hamory BH (1969) The minimal infectious dose of adenovirus type 4; the case for natural transmission by viral aerosol. *Trans Am Clin Climatol Assoc* 80:205–11.
18. Press Release – Novavax Available at: <http://ir.novavax.com/phoenix.zhtml?c=71178&p=irol-newsArticle&ID=2078538> [Accessed October 30, 2015].
19. Modjarrad K, Giersing B, Kaslow DC, Smith PG, Moorthy VS (2015) WHO consultation on

Respiratory Syncytial Virus Vaccine Development Report from a World Health Organization Meeting held on 23-24 March 2015. *Vaccine*. doi:10.1016/j.vaccine.2015.05.093.

20. Moorthy V, et al. WHO Consultations on RSV Vaccines and Passive Immunization.
21. Influenza Vaccination Coverage | FluVaxView | Seasonal Influenza (Flu) | CDC Available at: <http://www.cdc.gov/flu/fluview/> [Accessed August 8, 2016].
22. Mossong J, et al. (2008) Social contacts and mixing patterns relevant to the spread of infectious diseases. *PLoS Med* 5(3):e74.
23. Medlock J, Galvani AP (2009) Optimizing influenza vaccine distribution. *Science* 325(5948):1705–8.
24. Ibuka Y, et al. (2015) Social contacts, vaccination decisions and influenza in Japan. *J Epidemiol Community Health*:jech-2015-205777–.
25. DeVincenzo J, et al. (2010) A randomized, double-blind, placebo-controlled study of an RNAi-based therapy directed against respiratory syncytial virus. *Proc Natl Acad Sci U S A* 107(19):8800–5.
26. DeVincenzo JP, et al. (2014) Oral GS-5806 activity in a respiratory syncytial virus challenge study. *N Engl J Med* 371(8):711–22.
27. Fairchok MP, et al. (2010) Epidemiology of viral respiratory tract infections in a prospective cohort of infants and toddlers attending daycare. *J Clin Virol* 49(1):16–20.
28. Hall CB, Douglas RG, Geiman JM (1976) Respiratory syncytial virus infections in infants: Quantitation and duration of shedding. *J Pediatr* 89(1):11–15.
29. Hall CB, Douglas RG (1975) Clinically Useful Method for the Isolation of Respiratory Syncytial Virus. *J Infect Dis* 131(1):1–5.
30. Lessler J, et al. (2009) Incubation periods of acute respiratory viral infections: a systematic review. *Lancet Infect Dis* 9(5):291–300.
31. Taylor G, et al. (2015) Efficacy of a virus-vectored vaccine against human and bovine respiratory syncytial virus infections. *Sci Transl Med* 7(300):300ra127.
32. Grohskopf L, et al. (2013) *Prevention and Control of Seasonal Influenza with Vaccines: Recommendations of the Advisory Committee on Immunization Practices — United States, 2013–2014* Available at: http://www.cdc.gov/mmwr/preview/mmwrhtml/rr6207a1.htm?s_cid=rr6207a1_w [Accessed January 5, 2014].
33. FluView Interactive | Seasonal Influenza (Flu) | CDC Available at: <http://www.cdc.gov/flu/weekly/fluviewinteractive.htm> [Accessed October 30, 2015].
34. NREVSS | RSV Surveillance Data | CDC Available at: <http://www.cdc.gov/surveillance/nrevss/rsv/index.html> [Accessed October 30, 2015].
35. Zambon MC, Stockton JD, Clewley JP, Fleming DM (2001) Contribution of influenza and respiratory syncytial virus to community cases of influenza-like illness: an observational study. *Lancet (London, England)* 358(9291):1410–6.
36. Falsey AR, Hennessey PA, Formica MA, Cox C, Walsh EE (2005) Respiratory syncytial virus infection in elderly and high-risk adults. *N Engl J Med* 352(17):1749–59.
37. Burnham KP, Anderson DR, Burnham KP (2002) *Model selection and multimodel inference : a*

practical information-theoretic approach (Springer).

38. Wallinga J, Teunis P (2004) Different epidemic curves for severe acute respiratory syndrome reveal similar impacts of control measures. *Am J Epidemiol* 160(6):509–16.
39. Yamin D, et al. (2015) Effect of ebola progression on transmission and control in liberia. *Ann Intern Med* 162(1):11–7.